©2012

Elias Selwan

CONTROL STRATEGIES FOR POWER CONVERTERS USED ON SOLAR

CELLS

by

ELIAS SELWAN

A Thesis submitted to the

Graduate School-New Brunswick

Rutgers, The State University of New Jersey

in partial fulfillment of the requirements

for the degree of

Master of Science

Graduate Program in Electrical and Computer Engineering

written under the direction of

Dr. Zoran Gajic

and approved by

_____

_____

_____

_____

New Brunswick, New Jersey

October, 2012

ABSTRACT OF THESIS

Control Strategies for Power Converters used On Solar Cells

By ELIAS SELWAN

Thesis Director:

Zoran Gajic

The sun is considered as the major source of energy to the human kind from the beginning of life. This energy is radiated to earth by means of light and heat. We have been harnessing the solar energy for centuries and decades. The world is facing, especially in the recent years, a tremendous increase of energy demand from Asian to European and growing American countries as well as the traditional high energy demand from industrial countries. One solution to these problems is becoming so obvious, mass production and use of electricity generated from renewable energy especially solar energy, which is environmentally friendly. There are important applications of solar cells under development that directly relate to the field of power electronics, making ground for new opportunities in applications for low, medium and high power, for both DC and AC systems. High costs of conversion efficiency have been the major inconvenience in the potential of solar power becoming a primary source of energy. In our days, major researches done with the motive of improving the efficiency of these cells has brought this dream closer to reality. The technology proposed in this thesis is based on the idea that it is much more cost-effective to improve the solar cells by incorporating a smart control of power electronics than to improve the efficiency of the solar cells material by itself.

The thesis came across a new idea of simulating the Cuk converter using estimation techniques with full and reduced-order observers adding to them the integral action to

make the converter more and more competent. Great results were demonstrated with a very high performance.

The thesis also presents two major and efficient control algorithms for the Maximum Power Point Technique (MPPT); fuzzy logic control and its high reliability with very dynamic and weather related systems and the jump parameter linear control technique with an efficient algorithm.

Dedication

This thesis is dedicated to the memory of my father, Jean Selwan who always pushed me to exceed all expectations and who helped me aim high and get the best out of me. He taught me that the skies are my limit and that diligence and perseverance are the keys to any achievement and success. He believed in me and in what I can accomplish and his words of inspiration and support still linger on.

I miss you and love you so much dad. I wish you were here with me in these days so you can be proud of me. You will be always on my mind!!!

Acknowledgment

"What we do in Life… Echoes in Eternity" this quote was always the key motivator for any decision I make and any step I take. This master thesis writing process was a huge learning experience in my academic life which was filled with many challenges and wonderful achievements.

First, I would like to express my sincere gratitude to my advisor Dr. Zoran Gajic for his valuable guidance, opportunities and support which he presented to me during my graduate master's program at Rutgers University. I am grateful to Dr. Gajic for his immense knowledge and discussions on various topics that improved my thesis. The knowledge and experience gained by me while working under him are immeasurable.

I would like to thank my thesis committee members Dr. Ehab Shoubaki, Dr. Sigrid McAfee and Dr. Jingang Yi for their help, taking time out of their busy schedule to review my thesis work and their valuable advices.

I would like also to thank my entire family for always being next to me. Knowing that they always held me in their thoughts and prayers is what gave me strength to move forward. Special thanks to my aunts Amal Burlak and Noelle Andrea for their wonderful love, help and constructive advices. Great thanks to my mother Amal Selwan who has shown me the real meaning of the unconditional love. I would like to extend my appreciation towards my sister; Rita who has always been helpful in all my endeavors; and my friends Christian and Philippe Chemaly, and Antoine Chamoun for their continuous encouragements and for the fun times that we spent together.

Table of Contents

List of Figures

Chapter 1. Introduction

1.1   Overview

The sun is considered as the major source of energy to human kind from the beginning of life. This energy is radiated to earth by means of light and heat. We have been harnessing the solar energy for centuries and decades. This energy is considered as the oldest discovery in the renewable energy field. Photovoltaic cells (PV) is the field in which new technologies and applications are being researched and implemented in order to convert the light radiated by the sun into a more usable forms: electrical and heat power [1].

The world is facing, especially in the recent years, a tremendous increase of energy demand from Asian to European and growing American countries as well as the traditional high energy demand from industrial countries. This increase in the demand of energy has many undesirable effects [2]:

- First, oil prices have doubled in the last decade, increasing from 40 USD/barrel in 2002 to over 110 USD/barrel in the beginning of 2011. In addition, there is a forecast that fossil fuel will still be available in 2040, but there will be a geographical imbalance impact between the energy supply and demand that will eventually lead to the exhaustion of fossil fuels.

- Second, greenhouse effects and environmental threats are arising from the production of electricity from fossil fuels. The climate changes and global warming can cause floods and desertification over the world. With more lightly effects, the long dry periods will lower water levels in hydro-

electric facilities and may cause instability of the main electricity supply source in many countries.

One solution to these problems is becoming so obvious, mass production and use of electricity generated from renewable energy especially solar energy, which is environmentally friendly. So the world moved to start a dramatic increase in the production of photovoltaic cells, almost doubling every two years since 2002, making it the world's fastest-growing energy source (see Figure 1.1) that has so many benefits beside the clean energy production and inexhaustible supply of daylight. The solar photovoltaic (PV) systems can supply energy without moving parts, operate noiselessly and have minimum maintenance cost.
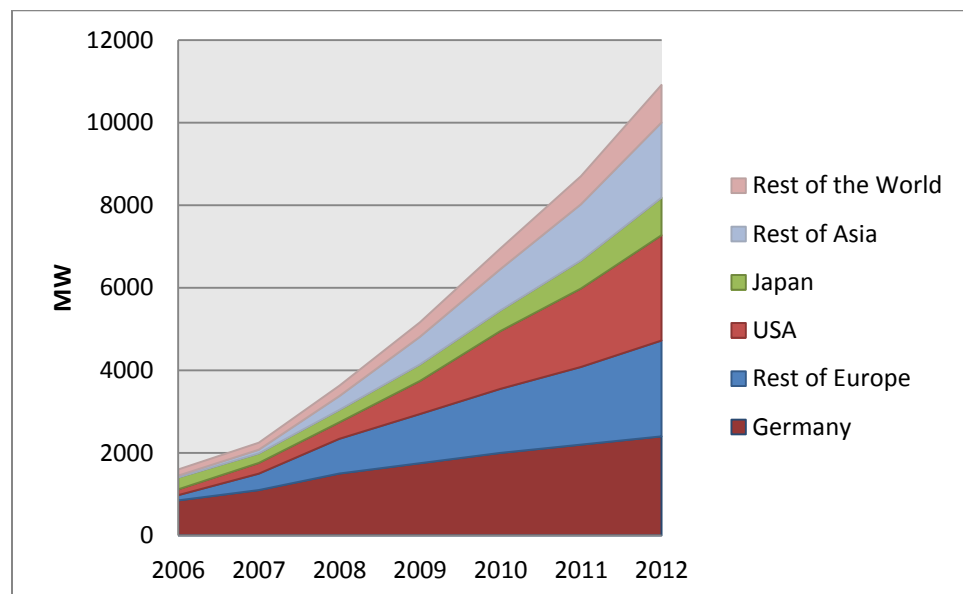
Figure 1.1 Global PV market

The cost trend of photovoltaic is downwards, while fossil fuel price are rising. The cost of PV modules and associated system components depend on developing mass production techniques and facilities. A growing and stable market of PV system is developing. Figure 1.1 shows the previous data of the

global market of PV to 2012. The total Mega Watt Power of global solar PV market is doubled for the period from 2009 to 2011. This growth in production and proliferating consumer demand has led to a world-wide interest in the development of new applications for photovoltaic technologies [3].

If we take a look at the National Renewable Energy Laboratory (NREL) data and illustrations, we notice that commercial photovoltaic cells, dependent on the price, have efficiencies between 10–22% in ordinary sunshine.

The cells are usually linked in series and fixed within weather-proof modules, with modules producing about 16 or 32 V. The current from the cell or module is inherently direct current, DC. And for a given module in an optimum fixed position, daily output depends on the climate, but can be expected to be about 0.5 to 1.0 kWh /m^2 day^{-1}. Output can be increased using tracking devices and solar concentrators [3].

1.2 Thesis Objective

There are two important applications of PV under development that directly relate to the field of power electronics, making ground for new opportunities in applications for low, medium and high power, for both DC and AC systems:

1.) The first area of research is in low-cost thin film solar cells. Due to their reduced material, energy and handling costs these could be a cost competitive product even without economic subsidies. Theoretically, these can be fabricated and even printed as a flexible and low-weight, yet thin and durable material. Film technologies are being developed in the form of semi-transparent cells to be applied as window glazing.

2.) The second large potential market is a new area where solar cells become architectural elements and building materials for residential and commercial structures.

High costs of conversion efficiency have been the major inconvenience in the potential of solar power becoming a primary source of energy. In our days, major researches done with the motive of improving the efficiency of these cells has brought this dream closer to reality.

The technology proposed in this thesis is based on the idea that it is much more cost-effective to improve the PV systems by incorporating a smart control strategy on the power electronics part than to improve the efficiency of the PV material by itself.

Chapter 2. Photovoltaic Cells

2.1   Photovoltaic Cells in Operation

To understand the electrical behavior of solar cells, it is useful to create an equivalent model, which is based on electrical components whose behavior is well known. A solar cell, also known as a photodiode, may be modeled by a current source in parallel with a diode. The diode in the model represents a real physical diode which is created by the junction of P and N materials which form the solar cell. As photons strike the cell's surface, they excite electrons and move them across the PN junction of the diode. Shunt and series resistances are added to obtain a better modeling of the current-voltage characteristic [5].

When the photovoltaic (PV) cell is illuminated and connected to a load a potential difference (V) appears across the load and a current (I) circulates. The cell functions as a generator as shown in Figure 2.3. The photons reaching the interior of the cell with energy greater than the band gap generate electron-hole pairs that may function as current carriers.
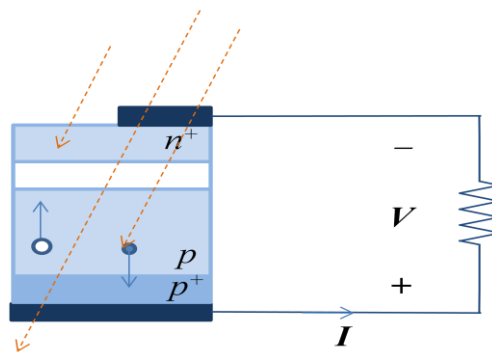
Figure 2.1 Illuminated PV cell

Some of these carriers will find themselves in or near the potential barrier and are accelerated as shown to form the photonic current.

Other carriers will recombine and contribute to a diode or dark current as governed by the Shockley equation:

$$I_D = I_0 (\exp(-V_D/m V_T) - 1) \tag{2.1}$$

With:

I_D : the diode current,

I_0 : the reverse bias saturation current (or scale current),

V_D : the voltage across the diode,

V_T : the thermal voltage,

m : the ideality factor, also known as the quality factor or sometimes emission coefficient. The ideality factor m varies from 1 to 2 depending on the fabrication process and semiconductor material and in many cases is assumed to be approximately equal to 1 (thus the notation m is omitted).

The thermal voltage V_T is approximately 25.85 mV at 300 K, a temperature close to "room temperature" commonly used in device simulation software. At any temperature it is a known constant defined by: $V_T = \frac{kT}{q}$, where k is the Boltzmann constant, T is the absolute temperature of the p–n junction, and q is the magnitude of charge on an electron (the elementary charge) [6].

The load current is the difference between the photonic and diode currents such that $I = I_v - I_D$ which when combined with Eq. 2.1 yields:

$$I = I_v - I_0 (\exp(-(V+IR_S)/m V_T) - 1) \tag{2.2}$$

<u>Note</u> V+IR$_S$ =V$_D$ and that the constant m= 1 at high current and m=2 at low current.

The saturation current I$_0$ is difficult to measure and the I-V equation may be more usefully written in terms of the open-circuit voltage (V$_{oc}$) and the short circuit current (I$_{sc}$).

The short circuit current is nearly equal to the photonic current I≈ I$_{sc}$ (R$_S$ is very small) and at open-circuit conditions reduces to:

$$0= I_{sc} – I_0 \, (exp \, (-(V_{oc})/V_T) – 1) \quad (2.3)$$

$$\Rightarrow$$
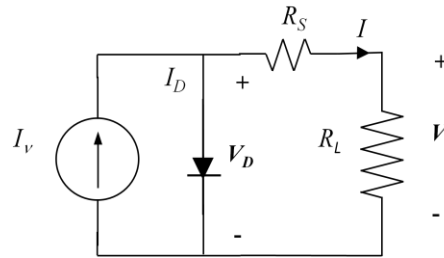
$$V_{oc} = V_T \; ln \, (I_{sc}/ I_0 + 1) \quad (2.4)$$

Figure 2.2 PV cell electric model

2.2   Photovoltaic Cells I-V Characteristics

A very useful expression (Eq. 2.5) of the I-V characteristic is obtained from equations 2.2, and 2.4:

$$V= V_{oc} + V_T \; ln \, (1 – I/I_{sc}) – IR_s \quad (2.5)$$

The above equation may be used to plot the I-V characteristic at different solar irradiance levels [7].
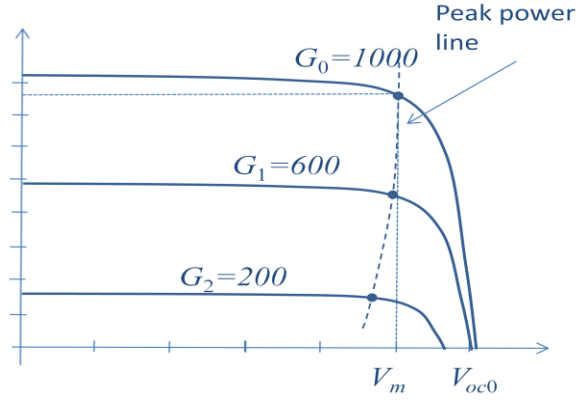
Figure 2.3 I-V characteristic

The open-circuit and short-circuit tests are usually given by manufacturers at standard conditions: G_0= 1000 W.m^{-2} and T_0= 20°C. Typical values are V_{oc0}=0.609V and I_{sc0}= 8.21A for a PV cell with a surface area A= 0.0243 m^2.

At another irradiance level G the photonic current and thus I_{sc} is given by:

$$I_{sc} = (G/G_0)\ I_{sc0} \tag{2.6}$$

The dependence of V_{oc} on solar irradiance may be written as:

$$V_{oc} = V_{oc0} + V_T \ln (G/\ G_0) \tag{2.7}$$

2.3   Photovoltaic Cells Efficiency

The maximum power at any solar irradiance is P_m= $V_m\ I_m$ is delivered from the PV cell when the equivalent load resistance is ideally matched such that R_L= V_m/I_m. As the solar irradiance changes then the values of V_m and I_m will change and to take maximum power from the cell the effective load resistance has to be changed using special switching DC-DC converters [6].

The efficiency at the maximum point, at any irradiance, is given by:

$$\eta_m= V_m\ I_m\ /\ G\,A \tag{2.8}$$

At lower solar irradiances the efficiency decreases.

The efficiency of a PV cell decreases with an increase in cell temperature. Eq. 2.5 suggests that as V_{oc} increases then V_m also increases. The dependence of V_{oc} is obtained by differentiating Eq. 2.4 after replacing $I_0 = A\Lambda n_i^2$ which yields:

$$dV_{oc} / dT = (k/q) (V_{oc} /V_T - 3 - V_g /V_T) \tag{2.9}$$

The value of the derivative is usually negative!

The cell temperature (T_C) depends only on the ambient temperature and solar irradiance as follows: $T_C = C_T G + T_a$, where $C_T = (NOCT - 20)/ 800$ and NOCT is the Normal Operating Cell Temperature given by a manufacturer test ($\approx 46°C$).

2.4   Photovoltaic Cells in Connections

Identical modules may be connected in series and parallel to form generators and are in general assumed to work under the same conditions of ambient temperature and irradiance. But operating conditions, however, may differ from some modules to other due to manufacturing differences, different accumulation of dirt, or shading. In such cases the maximum power delivered by the generator is less than the sum of the maximum powers of individual modules. This difference is named mismatch loss. There are also other undesired effects of the shadows on solar PV arrays other than power drop. Dynamic modeling of the effect of clouds on solar array is a difficult task. Cloud conditions can dramatically change fast and the cost of such fluctuations with their effect on other systems is important to understand [7].

A shadowed solar cell acts like a load dissipating power produced by others. In the presence of shadows, where there is no exposure to sunlight, a solar cell will heat up and develop a hot spot. So under these conditions the cell with

low current will experience a reverse bias and has to dissipate the power generated by the high current cells or modules.

1.) The most common technique used to avoid these hot spots is to connect bypass diodes in anti-parallel with a string of cells, thus any reverse bias is bypassed by the diodes. The bypass diodes are needed if the output voltage is larger than 24 V.

When the PV series string is operating under non-uniform conditions of radiation, a problem arises. All the cells in the system share the same current, and when a cell or group of cells is shaded one of two scenarios may occur:

a. The group of shaded cells will try to drive the unshaded ones into operating at a lower current level. In this case the system output power is limited by the current produced by the cell or panel generating the lowest output current.

b. The unshaded cells will try to drive the shaded ones into operating at a higher current level. The only way a PV cell can operate at a higher current than its short circuit current, which is directly proportional to irradiance, is by moving into the negative voltage region of the cell's I-V curve where it becomes reverse biased. At this point the panel's backplane diode(s) becomes forward biased and it conducts the string current. The down side is that now the group of shaded cells is entirely bypassed, contributing zero power to the system, and the string voltage is also affected.

2.) A similar analysis reveals that when modules are connected in parallel, the module with lower V_{oc} will be come a load dissipating power generated by other modules with higher open circuit voltage. The problem is avoided by connecting blocking diodes in series with each of the parallel modules.

Chapter 3. Cuk Converter

3.1 Cuk Converter Circuit

The buck, boost and buck-boost converters all transfer energy between input and output using an inductor, and analysis is based on the inductor voltage balance. The Cuk converter uses capacitive energy transfer and analysis can be based on current balance of the capacitor (although inductor voltage-balance analysis is also valid). The Cuk converter combines the functionality of a buck and boost converters, i.e. it can increase or decrease the output voltage with respect to the input voltage. It uses a capacitor as its main energy-storage component, which increases its efficiency. Input and output currents are smoothed by inductors.
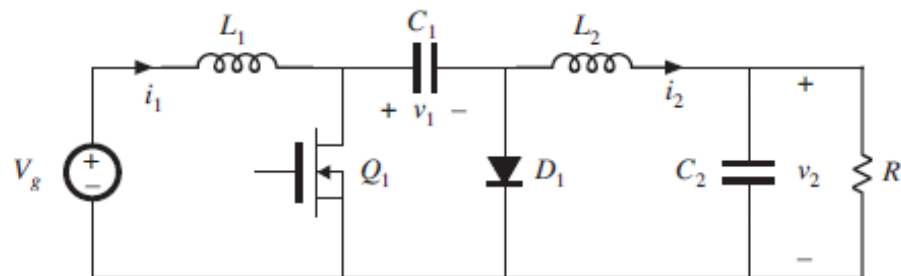
Figure 3.1 Cuk converter

Virtually all of the output current must pass through C_1, so it is usually a capacitor with a high ripple current rating and low equivalent series resistance (ESR), in order to minimize as much as we can the losses [8]. When the switch Q_1 is at "ON-STATE" (see Figure 3.2), the current flows from the input source through L_1, and storing energy in L_1's magnetic field. Then, when Q_1 switch is at "OFF-STATE" (see Figure 3.3), the voltage across L_1 reverses to maintain current flow. Current flows from the input source, through L_1 and D_1,

charging up C_1 to a voltage larger than in V_2, and transferring to it some of the energy that was stored in L_1.

Then when Q_1 is turned on again, C_2 discharges through via L_2 into the load (in this case it is a resistive load R), with L_2 and C_2 acting as a smoothing filter. Meanwhile energy is being stored again in L_1, ready for the next cycle. In steady state, the voltage across C_1 is $(|V_g|+|V_2|)$, which means the switch and the diode in a Cuk converter must handle larger voltages than what is the case for the regular buck and boost converters.
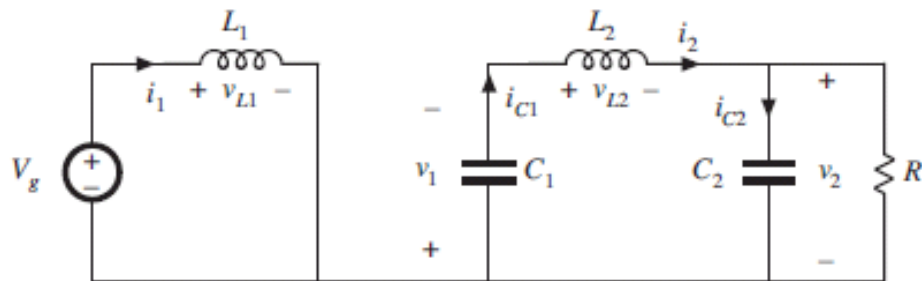
Figure 3.2 Cuk converter with Q1 "ON-STATE"
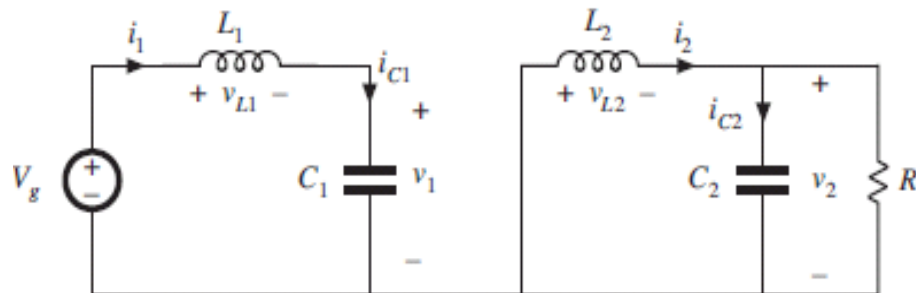
Figure 3.3 Cuk converter with Q1 "OFF-STATE"

The energy stored in an inductor is given by:

$$E= \tfrac{1}{2} LI^2 \tag{3.1}$$

L does not change and in steady state the energy has to remain the same at the start or end of commutation cycle, which implies that the current through the

inductors has to be the same at the beginning and the end of the commutation cycle.

The current through an inductor is related to the voltage across it, which is given by the following formula:

$$V_L = L\, dI/dt \qquad\qquad (3.2)$$

Note: The average value of the inductor voltage over a commutation period has to be zero to satisfy the steady-state requirements.

If we consider that the capacitors C_2 and C_1 are large enough for the voltage ripple across them to be negligible, the inductor voltages become:

1.) In the "OFF-STATE", inductor L_1 is connected in series with V_g and C_1. Therefore $V_{L1} = V_g - V_{C1}$. As the diode D_1 is forward biased (we consider zero voltage drop), L_2 directly connected to the output capacitor. Therefore $V_{L2} = V_2$.

2.) In the "ON-STATE", inductor L_1 is directly connected in series to V_g. Therefore $V_{L1} = V_g$. Inductor L_2 is connected in series with C_1 and the output capacitor. Therefore $V_{L2} = V_2 - V_{C1}$.

The Q_1 switch operates in "ON-STATE" from $t = 0$ to $t = \Gamma T$ (with Γ the duty cycle of the switch with $0 < \Gamma < 1$), and in "OFF-STATE" from ΓT to T (that is, during a period equal to $(1-\Gamma)\,T$). The average values of V_{L1} and V_{L2} are therefore:

$$\overline{V}_{L1} = \Gamma\, V_g + (1-\Gamma)(V_g - V_{C1})$$

$$\qquad\qquad (3.3)$$

$$\overline{V}_{L2} = \Gamma\, (V_2 - V_{C1}) + (1-\Gamma)(V_2)$$

As both average voltages have to be zero to satisfy the steady-state conditions we can write, using (3.3):

$$V_{C1} = V_2 / \Gamma \qquad (3.4)$$

Therefore we have:

$$\Rightarrow \overline{V}_{L1} = \Gamma V_g + (1 - \Gamma)(V_g - V_{C1}) = 0 = V_g + (1 - \Gamma)(V_2 / \Gamma)$$

$$\Rightarrow \quad \frac{Vg}{V2} = -\frac{\Gamma}{1 - \Gamma} \qquad (3.5)$$

It can be noticed that this relation is the same as that obtained for the Buck-Boost converter.

The advantage of the Cuk converter is that the input and output inductors create a smooth current at both sides of the converter while the buck, boost, buck-boost and even the Single-ended primary-inductor (SEPIC) have at least one side with pulsed current. Also Cuk has a simple implementation that requires fewer parts and simpler drive circuitry comparing to the other converters.

Ideally the Cuk converter provides excellent frequency response characteristics which allow a highly stable feedback regulation to be achieved.

3.2   Cuk Converter State-Space Analysis

We assume ideal components, so we have continuous current conduction and continuous capacitor voltage. There are 2 modes of operation [9]:

    1.) In mode 1: Q_1 is on and D_1 is off

    2.) In mode 2: Q_1 is off and D_1 is on

The state variables are:

$$\begin{bmatrix} x_1 \\ x_2 \\ x_3 \\ x_4 \end{bmatrix} = \begin{bmatrix} i_{L1} \\ i_{L2} \\ v_{C1} \\ v_{C2} \end{bmatrix} \tag{3.6}$$

Mode 1

By applying KVL and KCL to the above circuit, the state equations are determined.

The loop and node equations are:

$$-V_g + V_{L1} = 0$$

$$I_{C1} = -I_{L2}$$

$$V_{C1} - V_{L2} - V_{C2} = 0 \tag{3.7}$$

$$I_{C2} = I_{L2} - I_R$$

$$I_R = \frac{V_{C2}}{R}$$

Now, the state equations are:

$$\frac{di_{L1}}{dt} = \frac{1}{L_1} V_g$$

$$\frac{dv_{C1}}{dt} = -\frac{1}{C_1} i_{L2} \tag{3.8}$$

$$\frac{di_{L2}}{dt} = \frac{1}{L_2} V_{C1} - \frac{1}{L_2} V_{C2}$$

$$\frac{dv_{C2}}{dt} = \frac{1}{C_2} i_{L2} - \frac{1}{RC_2} V_{C2}$$

$$v_2 = v_{C2}$$

The state-space system in mode 1 becomes:

$$\dot{x} = \begin{bmatrix} 0 & 0 & 0 & 0 \\ 0 & 0 & \frac{1}{L_2} & -\frac{1}{L_2} \\ 0 & -\frac{1}{C_1} & 0 & 0 \\ 0 & \frac{1}{C_2} & 0 & -\frac{1}{RC_2} \end{bmatrix} x + \begin{bmatrix} \frac{1}{L_1} \\ 0 \\ 0 \\ 0 \end{bmatrix} V_g \tag{3.9}$$

$$v_2 = [0 \quad 0 \quad 0 \quad 1]x = G_1 x \tag{3.10}$$

Mode 2

Similarly in mode 2 we determine the following state equations:

$$\frac{di_{L1}}{dt} = \frac{1}{L_1} v_g - \frac{1}{L_1} v_{C1}$$

$$\frac{dv_{C1}}{dt} = \frac{1}{C_1} i_{L1}$$

$$\frac{di_{L2}}{dt} = -\frac{1}{L_2} v_{C2} \tag{3.11}$$

$$\frac{dv_{C2}}{dt} = \frac{1}{C_2} i_{L2} - \frac{1}{RC_2} v_{C2}$$

$$v_2 = v_{C2}$$

The state-space system in mode 2 becomes:

$$\dot{x} = \begin{bmatrix} 0 & 0 & -\frac{1}{L_1} & 0 \\ 0 & 0 & 0 & -\frac{1}{L_2} \\ \frac{1}{C_1} & 0 & 0 & 0 \\ 0 & \frac{1}{C_2} & 0 & -\frac{1}{RC_2} \end{bmatrix} x + \begin{bmatrix} \frac{1}{L_1} \\ 0 \\ 0 \\ 0 \end{bmatrix} v_g \tag{3.12}$$

$$v_2 = [0 \quad 0 \quad 0 \quad 1]x = G_2 x \tag{3.13}$$

The averaged state space model is:

$$\dot{x} = Ax + Bv_g$$

$$v_2 = Gx$$

With

A= Γ A₁ + (1– Γ)A₂

B= Γ B₁ + (1– Γ)B₂

G= Γ G₁ + (1– Γ)G₂

then

$$A = \begin{bmatrix} 0 & 0 & -\frac{1-\Gamma}{L_1} & 0 \\ 0 & 0 & \frac{\Gamma}{L_2} & -\frac{1}{L_2} \\ \frac{1-\Gamma}{C_1} & -\frac{\Gamma}{C_1} & 0 & 0 \\ 0 & \frac{1}{C_2} & 0 & -\frac{1}{RC_2} \end{bmatrix}; \; B = \begin{bmatrix} \frac{1}{L_1} \\ 0 \\ 0 \\ 0 \end{bmatrix} \qquad (3.14)$$

$$G = [0 \quad 0 \quad 0 \quad 1] \qquad\qquad D = 0 \qquad (3.15)$$

The steady state voltage transfer function:

$$\frac{v_2}{v_g} = GA^{-1}B = \frac{\Gamma}{1-\Gamma} \qquad (3.16)$$

Which confirms the analysis done using the voltage or current balance; in addition this analysis has the orientation of V_2 already reversed which is why we have a positive $\frac{\Gamma}{1-\Gamma}$.

3.3   Open-Loop Performance of Cuk Converter

Before we start with the controller design, we will study the open-loop performance of the Cuk converter. The state space equation can be written using the technique demonstrated by Middlebrook and Cuk [10] as:

$$\dot{x} = Ax + Bv_g + B_s\gamma$$

$$y = v_2 = Gx + H_s\gamma$$

where:

$$x = X + \tilde{x}$$

$$v_g = V_g + \tilde{v}_g$$

$$\gamma = \Gamma + \tilde{\gamma}$$

$$v_2 = V_2 + \tilde{v}_2$$

$$B_s = (A_1 - A_2)X + (B_1 - B_2)V_g = (A_1 - A_2)X$$

$$H_s = (G_1 - G_2)X = 0$$

Steady state system gives: $AX + BV_g = 0 \Rightarrow X = -A^{-1}BV_g$

With (˜) denotes small signal perturbation or deviation from the nominal or average value.
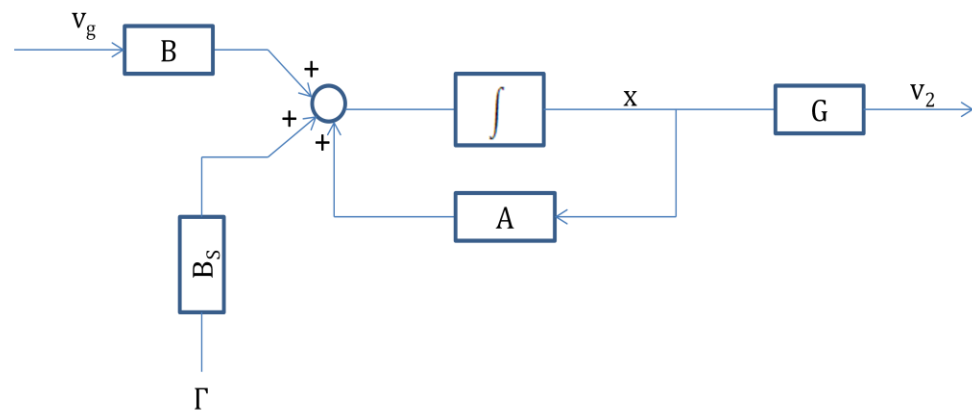
Figure 3.4 Cuk converter state-space model

The state space matrices for the open-loop model from the disturbance input v_g to the output v_2 are the state space averaged matrices (A, B, G, and H). The state space matrices for the open-loop system from the control input (switching duty cycle) d to the output v_2 are the state space averaged matrices (A, B_s, G, and H). The Cuk converter model can be shown as a two inputs (control input (the duty cycle γ) with a disturbance (input voltage v_g)) and one output (v_2). The model of the open-loop response to a unit step input (disturbance) in v_g is shown in Figure 3.5.

The graph (Figure 3.5) is based on the given circuit components standard values below (these values will be used in all the simulations and the cases treated later on):

$L_1 = 0.5mH$

$L_2 = 7.5mH$

$C_1 = 2.0 \ \mu F$

$C_2 = 20 \ \mu F$

$R = 30\Omega$

$V_g = 20V$

$\Gamma = 0.667$

As we can notice from the Figure 3.5 below, the system is slightly damped and presents oscillations around a steady state value equal to 42 Volts. If we apply the formula (3.15) with a nominal duty cycle $\Gamma = 0.667$, then the output voltage should be 40V. However, with the chosen Γ, and as we inspected from the graph, a 1V step input in v_g has produced a 2V step in the output voltage v_2. This shows that the open-loop system does not reject disturbances on the input voltage v_g. Also, we note that the output of the circuit is a damped sinusoid, with an approximate frequency of 1.9 kHz (12 krad / s).
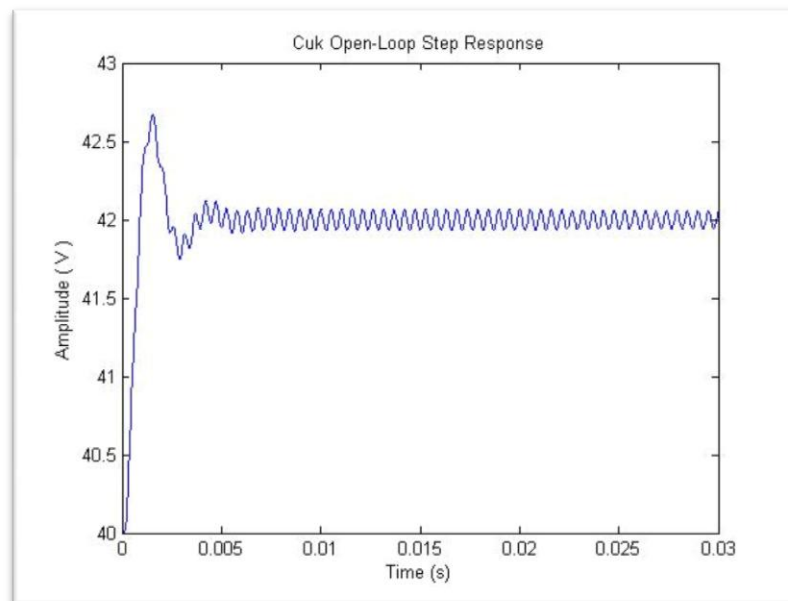
Figure 3.5 Cuk converter open-loop response
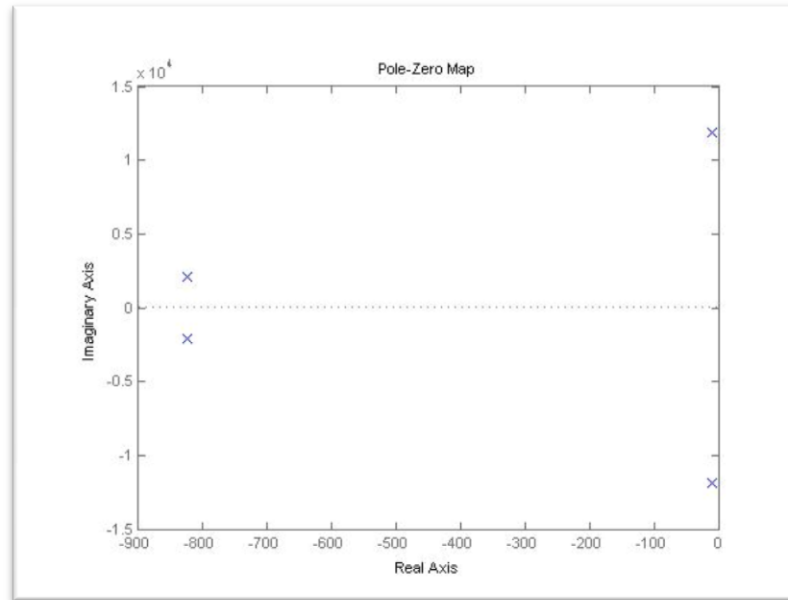
Figure 3.6 Cuk converter open-loop poles-zeros map
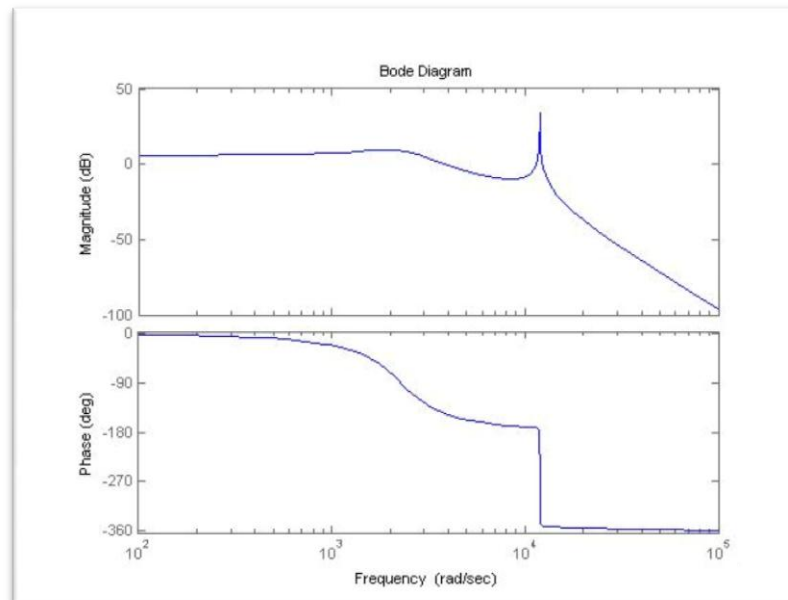
Figure 3.7 Cuk converter Bode diagram

The pole-zero mapping shows (see Figure 3.6) that the Cuk converter is stable; all the poles are in the left hand side. The 1.9 kHz frequency in the output, transient caused by the unit step disturbance, is due to the frequency associated with the dominant pole pair at: -8.69±j*0.19e+004.

3.4   Cuk Converter Analysis

Using MATLAB scripts we will vary the values of individual components and determine the damping and frequency of the system.

3.4.1   Inductors Effect:

Keeping all other components constant, L_1 and L_2 were varied from 1mH to 0.1mH and keeping them both with equal values.

L_1 and L_2 (H)	Damping 1	Frequency 1 (rad/s)	Damping 2	Frequency 2 (rad/s)
1.10^{-3}	2.45e-001	2.95e+003	6.17e-003	1.79e+004
9.10^{-4}	2.32e-001	3.11e+003	5.85e-003	1.88+004
6.10^{-4}	1.90e-001	3.81e+003	4.79e-003	2.31e+004
3.10^{-4}	1.34e-001	5.39e+003	3.39e-003	3.26e+004
1.10^{-4}	7.74e-002	9.33e+002	1.96e-003	5.65e+004

Table 3.1 Cuk converter parameter variations with inductance

As L_1 and L_2 decrease, the damping also decreases and the frequency of oscillation increases.

A small inductor will cause the inductor current to overshoot causing the voltage across it to overshoot almost 4V over the steady state value 42V as it is noticed in the Figure 3.8 below:

This can be easily explained by the fact that inductors L_1 and L_2 are used as smoothing inductors in the Cuk converter.
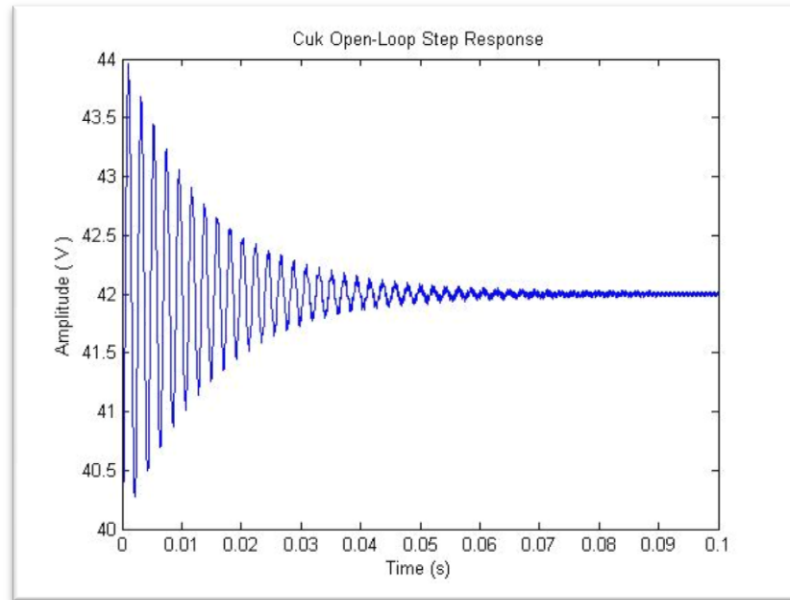
Figure 3.8 Cuk converter open-loop response with $L_1=L_2=0.1$ mH

3.4.2   Capacitors Effect:

If we take a look on the behavior of the converter while we fix the values of the inductance to $L_1=L_2=1$mH and we change the values of the capacitors.

It seems that lowering the values of C_1 and C_2 improves the response of the converter and it make the output goes smoothly to a constant value (see Figure 3.9) but an overshoot of the voltage still appear and it is around 0.5V and it will stabilize also at 42V.

Having large C_1 and C_2 will decrease the voltage ripple across the capacitor but on the other hand having chosen big values for C_1 and C_2, it has other drawbacks (see Figure 3.10). A larger capacitor value means less voltage ripple in steady state, which is good, however, it also causes an increase in overshoot and oscillations and it took much longer time for the voltage to stabilize around the 42V. Also if we lower C_1 and C_2 to a value less or equal to

0.5 µF we will have a damping ratio equal to 1 (critically damped system see Figure 3.11).
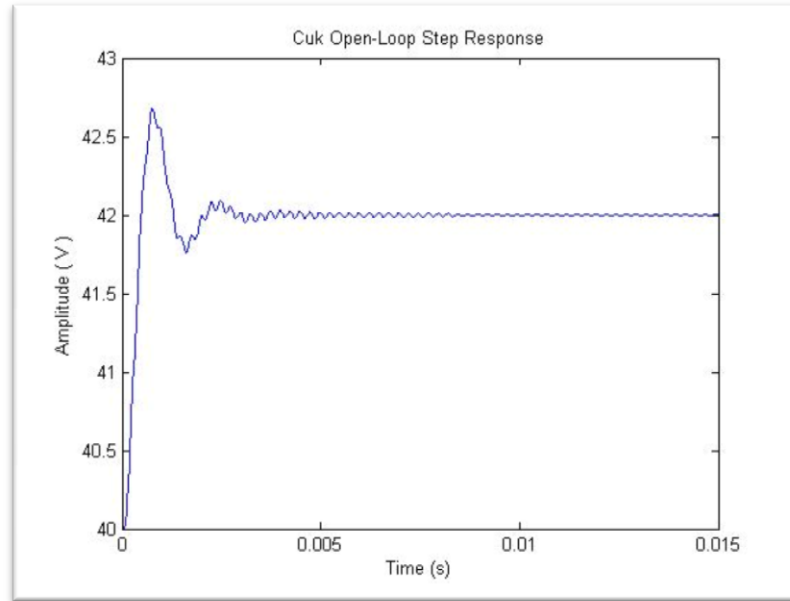
Figure 3.9 Cuk converter open-loop response with C1 =1µF and C2=10µF
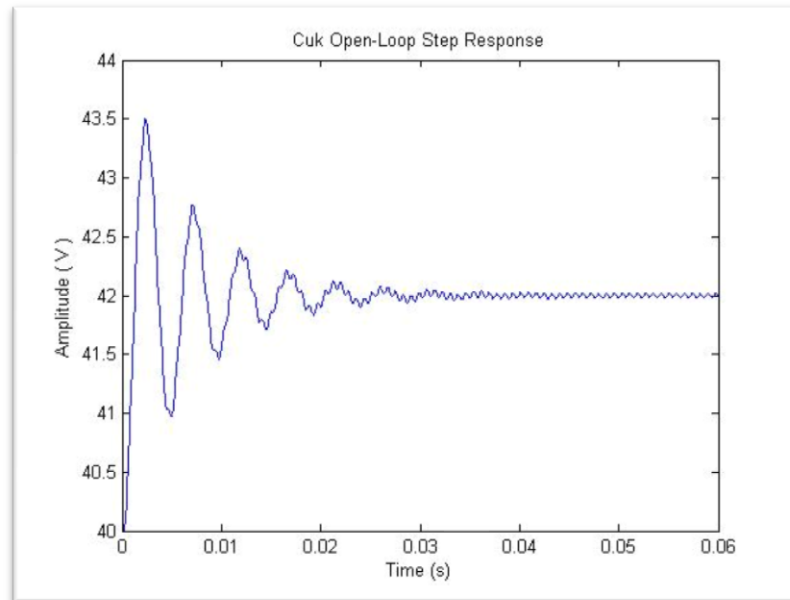
Figure 3.10 Cuk converter open-loop response with C1 =10µF and C2=100µF
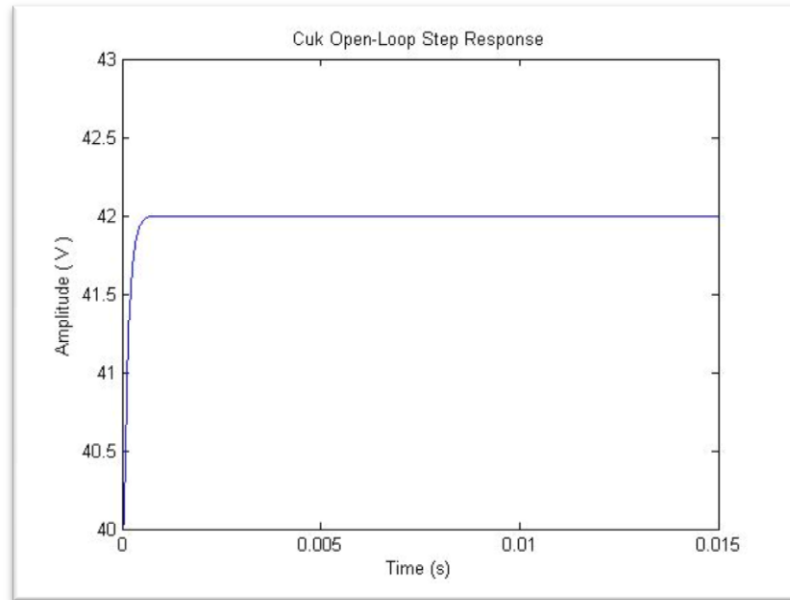
Figure 3.11 Cuk converter open-loop response with C1 = C2=0.5µF

After choosing a high value of C_2 (let's make it equal to 10mF), we inspected an almost 3 seconds time for the voltage to stabilize after high overshoot and high frequency oscillations (see Figure 3.10). But with a lower value of C_2 (equal to 1 mF) it needed 0.4 seconds for the converter to stabilize around the 42V with fewer oscillations but same overshoot value.
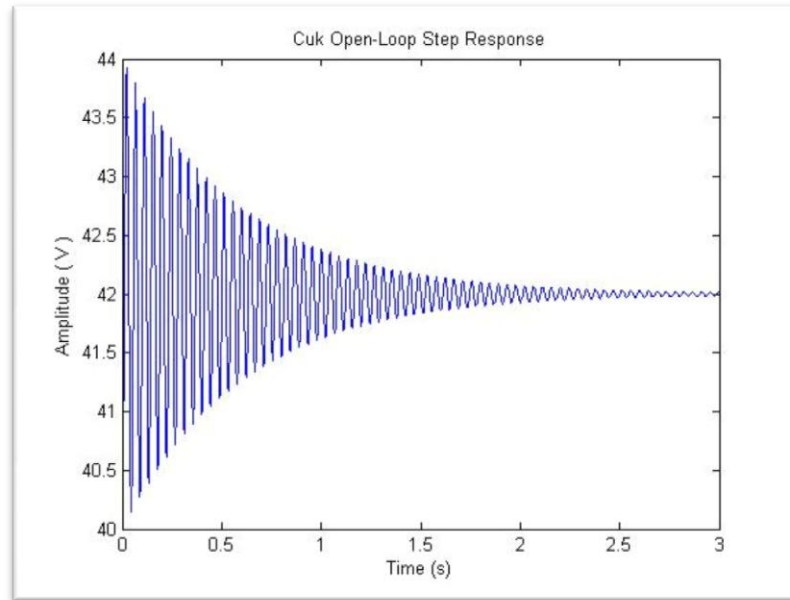
Figure 3.12 Cuk converter open-loop response with C2=10mF
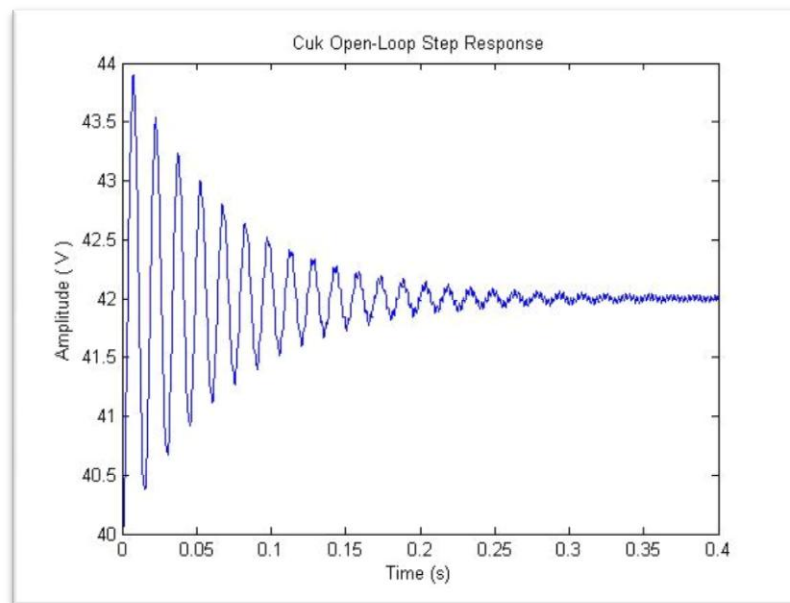
Figure 3.13 Cuk converter open-loop response with C2 = 1mF

3.5   Cuk Converter State Feedback Control

3.5.1.   Full State Feedback Controller with the Integral Action

The graphed responses in the previous section showed us that the Cuk converter is a stable system ((Aav, Bav) are chosen in a way that the system be controllable). However, 1V step disturbance in v_g has produced a 2V step in the output voltage v_2 showing that the Cuk system does not reject any kind of disturbances on the input voltage v_g. So in order to eliminate this offset we have thought about controlling the Cuk converter with a full state feedback controller with an integral action to remove the steady-state offset. The basic approach in integral action feedback is to create a state within the controller that computes the integral of the error signal, which is then used as a feedback term. In this way the integral action will integrate the error between any reference input and the output e(t)=r(t)-y(t) and add it to the state feedback control effort to eliminate the steady-state offset [11]. The control law is: $u = -Fx - f\varepsilon$ with $\varepsilon(t)$ the offset error with $\dot{\varepsilon}(t) = -y(t) = -Gx$. The state space model is shown below:
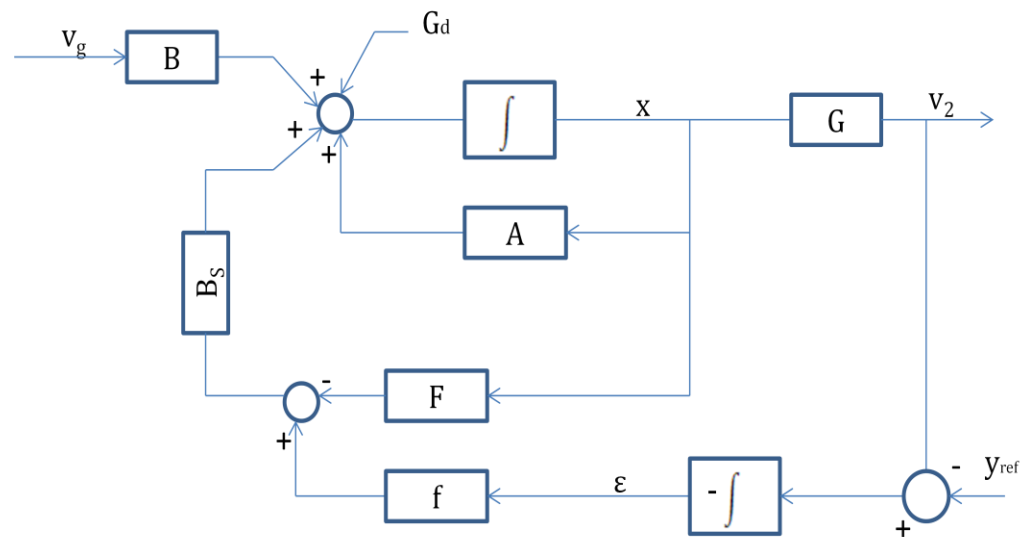
Figure 3.14 Cuk converter state feedback control with the integral action space model

So the state space matrices can be written as the following:

$$\begin{bmatrix} \dot{x} \\ \dot{\varepsilon} \end{bmatrix} = \begin{bmatrix} A_{av} - B_s F & -B_s f \\ G_{av} & 0 \end{bmatrix} \begin{bmatrix} x \\ \varepsilon \end{bmatrix} + \begin{bmatrix} B_{av} \\ 0 \end{bmatrix} v_g + \begin{bmatrix} G_d \\ -y_{ref} \end{bmatrix}$$

$$v_2 = \begin{bmatrix} G_{av} & 0 \end{bmatrix} \begin{bmatrix} x \\ \varepsilon \end{bmatrix}$$

With

$$A_l = \begin{bmatrix} A_{av} - B_s F & -B_s f \\ G_{av} & 0 \end{bmatrix}$$

$$B_l = \begin{bmatrix} B_{av} \\ 0 \end{bmatrix}$$

$$G_l = \begin{bmatrix} G_{av} & 0 \end{bmatrix}$$

$$H_l = \begin{bmatrix} H_{av} \end{bmatrix}$$

In order to determine the optimal pole placement for the system augmented with the integrator, we will try to create an optimum system by minimizing the Integral of Time Multiplied Absolute Error. A control system is optimal when the performance index J is minimized. The optimum value of the parameters depend directly upon the definition of what is optimum which is in our case the minimum performance index of the Integral of Time Multiplied Absolute Error $J_{ITAE} = \int t|\varepsilon(t)|dt$. [12]

The coefficients to minimize the performance are already calculated and tabulated in [12]. (See below):

- $s + \omega_n$

- $s^2 + 1.4\omega_n s + \omega_n^2$

- $s^3 + 1.75\omega_n s^2 + 2.15\omega_n^2 s + \omega_n^3$

- $s^4 + 2.1 \omega_n s^3 + 3.4 \omega_n^2 s^2 + 2.7 \omega_n^3 s + \omega_n^4$

- $s^5 + 2.8 \omega_n s^4 + 5.0 \omega_n^2 s^3 + 5.5 \omega_n^3 s^2 + 3.4\omega_n^4 s + \omega_n^5$

- $s^6 + 3.25\omega_n s^5 + 6.60 \omega_n^2 s^4 + 8.60\omega_n^3 s^3 + 7.45 \omega_n^4 s^2 + 3.95\omega_n^5 s + \omega_n^6$

We used n=5 for the coefficients and we have obtained a great results (see Figure 3.16) concerning the error elimination; also we have enhanced the Cuk converter to accommodate to any kind of disturbance by creating a closed loop with an integral action.

The program consists on running the frequency w_n from 1 to 15 rads/sec with a step of 0.01 rad/s (the more values we compute, the more our search is accurate and can lead us to reduce the error to be close more and more to zero). For each iteration we replace w_n by its value in the picked polynomial $P(s)=s^5 + 2.8\ \omega_n s^4 + 5.0\ \omega_n^2 s^3 + 5.5\ \omega_n^3 s^2 + 3.4\omega_n^4 s + \omega_n^5$ and then we do the pole placement and calculate the performance index.

The w_n corresponding to the minimum performance index is used to plot the output of the system with state-feedback with the integral action. In our case (Cuk parameters are chosen in the beginning of our study) the minimum performance index, equal is to $2*10^{-5}$, is reached for w_n=8.4 rad/s.
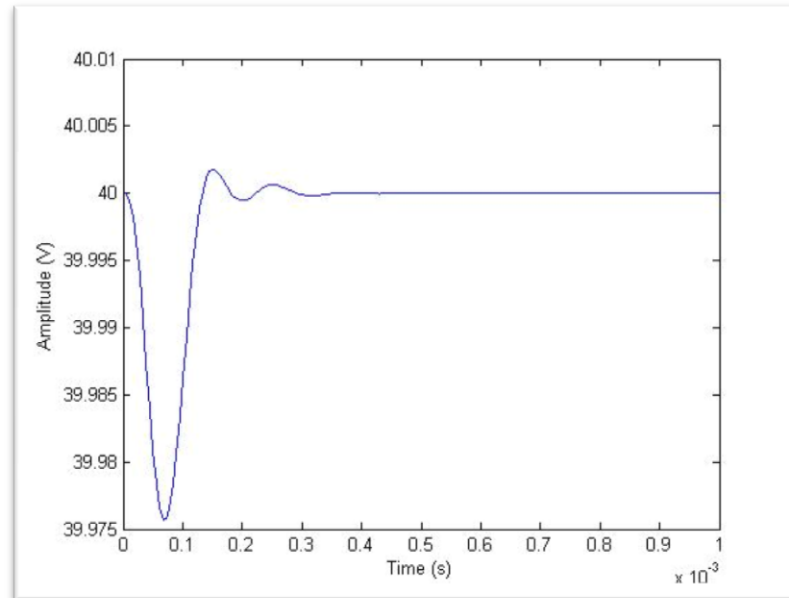
Figure 3.15 Cuk converter response with feedback control with the integral action

3.5.2. Linear Quadratic Regulator and Integrate Action

Linear Quadratic Regulators are introduced in the state feedback control in order to minimize a quadratic performance criterion. The regulator should reduce the performance index [13]:

$$J = \frac{1}{2} \int_0^\infty (x^T Q x + u^T R u) dt$$

with the state equation considered as a constraint $\dot{x} = Ax + Bu$. So the optimal value of the performance criterion is evaluated as below:

$$\dot{x} = Ax + Bu \qquad u = -kx \qquad x(0) = x_0$$

$$J = \min_u \frac{1}{2} \int_0^\infty (x^T Q x + u^T R u) dt$$

$$\dot{x} = (A - Bk)x \quad \text{with} \quad x(0) = x_0$$

$$x = e^{(A-Bk)t} x_0$$

If we now assume that we use optimal control, that is $u = u_{opt}$ given by [14]:

$$u = -R^{-1} B^T P x = -k_{opt} x$$

the performance criterion is:

$$J = \frac{1}{2} x_0^T \left(\int_0^\infty e^{(A-Bk_{opt})^T t} \left(Q + k_{opt}^T R k_{opt} \right) e^{(A-Bk_{opt})t} dt \right) x_0$$

it can be evaluated from the algebraic Lyapunov equation:

$$(A - Bk_{opt})^T P + P(A - Bk_{opt}) + \left(Q + k_{opt}^T R k_{opt} \right) = 0$$

Now if we have the optimal control then $k_{opt} = -R^{-1} B^T P x$

$$A^T P - PBR^{-1} B^T P + PA - PBR^{-1} B^T P + Q + PBR^{-1} B^T P = 0$$

$$\Rightarrow A^T P - PBR^{-1} B^T P + PA + Q = 0$$

This is the Riccati algebraic equation and the optimal performance criterion is:

$$J = \frac{1}{2} x_0^T P x_0$$

Now applying the optimal control to the Cuk converter, we first augment the converter control system to be a fifth order system with an integral state and this will also require that the weighting matrix Q be a five-by-five matrix.

For review, we have that the state vector is $[i_{L1} \ i_{L2} \ v_{C1} \ v_{C2} \ \varepsilon]'$, where ε corresponds to the integral of the reference error. Since the states have physical significance in this model, it is easy to see that each voltage, current, or error transient may be individually weighted using the diagonal elements of the Q matrix. As the objective of controlling the Cuk converter is to regulate the output v_2 in the face of disturbances to the input v_g.
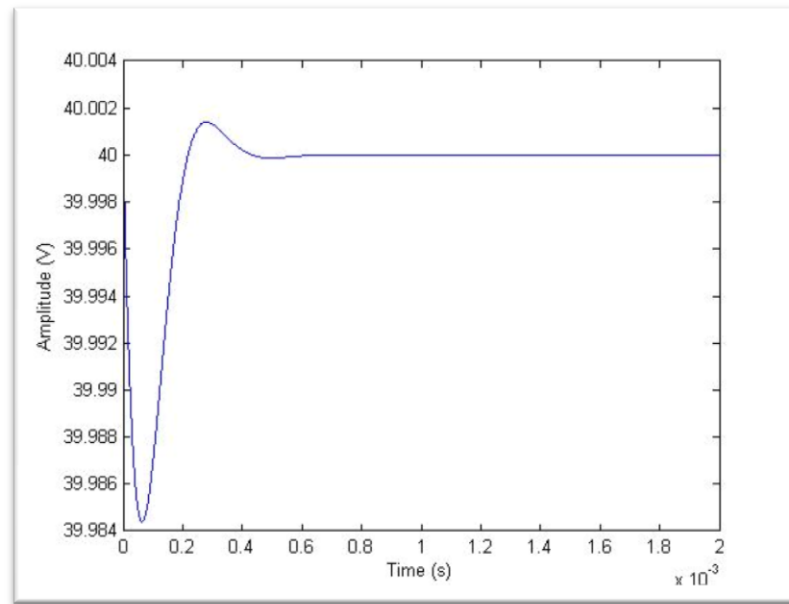
Figure 3.16 Cuk converter response with LQR regulator with the integral action

We have obtained some great results also and we were able to reduce the error in the Cuk converter output response for a disturbance in the input voltage with a linear quadratic regulator to a very minimal value highly desired.

3.5.3. <u>Full-Order Observer with the Integral Action</u>

a. <u>Full-Order Observer</u>

Not always we have that all the state space variables are available for measurements, or it is not practical to measure all of them, or it is too expensive to measure all state space variables. In order to be able to apply the state feedback control to a system, all of its state space variables must be available at all times. Thus, one is faced with the problem of estimating system state space variables.

This can be done by constructing another dynamical system called the observer or estimator, connected to the system under consideration, whose role is to produce good estimates of the state space variables of the original system. The output of the estimator $\hat{y} = C\hat{x}$ can be compared to the output of the system $y = Cx$ and any difference between them will be multiplied by a gain vector and fed back to the state estimator dynamics [15], see Figure 3.17.

The difference between these two outputs will generate an error signal:

$$y - \hat{y} = Cx - C\hat{x} = Ce$$

This error can be used as the feedback signal to the artificial system such that the estimation (observation) error is reduced as much as possible, hopefully to zero.
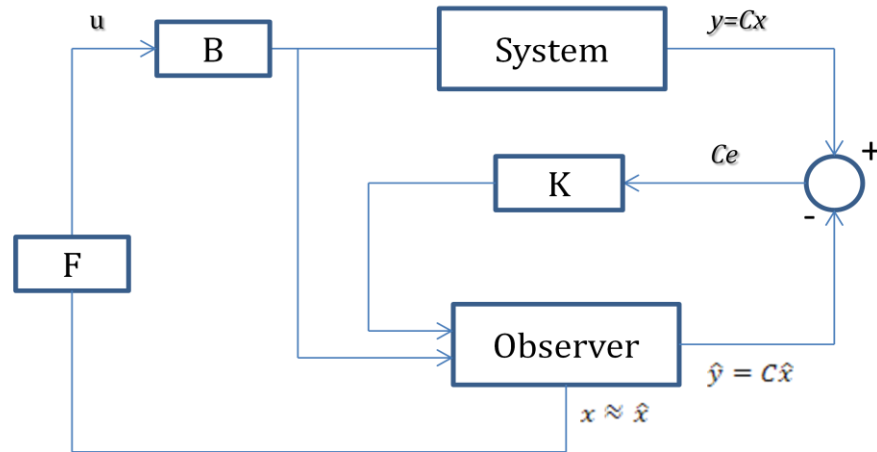
Figure 3.17 System and full-order observer block diagram

K is chosen in a way to minimize as much as possible the observation error.

The observer is then given by:

$$\dot{\hat{x}} = A\hat{x} + Bu + K(y - \hat{y})$$

$$\dot{\hat{x}} = A\hat{x} + Bu + KCe$$

We can write the observer's equation in the following form:

$$\dot{\hat{x}} = (A - KC)\hat{x} + Bu + Ky$$

with $\dot{e} = \dot{x} - \dot{\hat{x}} = (A - KC)e$

The system-observer structure preserves the closed-loop system poles that would have been obtained if the linear perfect state feedback control had been used (separation principle).

The system under the perfect state feedback control which is expressed as $u = -Fx$ and $\dot{x} = (A - BF)x$ and in the case of the system-observer structure, as given in Figure 3.17, we see that the actual control applied to both the system and the observer is given by : $u = -F\hat{x} = -Fx + Fe$

The system-observer's state-space matrices can be written:

$$\begin{bmatrix} \dot{x} \\ \dot{\hat{x}} \end{bmatrix} = \begin{bmatrix} A & -BF \\ KC & A - KC - BF \end{bmatrix} \begin{bmatrix} x \\ \hat{x} \end{bmatrix}$$

$$\begin{bmatrix} \dot{x} \\ \dot{e} \end{bmatrix} = \begin{bmatrix} A - BF & BF \\ 0 & A - KC \end{bmatrix} \begin{bmatrix} x \\ e \end{bmatrix}$$

b. <u>Cuk Converter with a Full-Order Observer with the Integral Action</u>

- Implementation:

Now if we take the system that we have implemented in Section 3.5.1 (Cuk converter with the integral action) and we augment it by taking care of the system-observer structure and using the formulas that we have determined in 3.5.3 part a, we will have the following:

The equations are given by the state space equation:

$$\dot{x} = A_{av}x - B_s F\hat{x} - B_s f\varepsilon + B_{av}v_g + G_d$$

and $y = G_{av}x$

The integral action is $\dot{\varepsilon} = y - y_{ref} = G_{av}x - y_{ref}$

We have also $\dot{\hat{x}} = Ky - B_s f\varepsilon - B_s F\hat{x} + A_{av}x - B_s F\hat{x} - Ky$

$\Rightarrow \dot{\hat{x}} = KG_{av}x - B_s f\varepsilon + A_{av}\hat{x} - B_s F\hat{x} - KG_{av}\hat{x}$

$\Rightarrow \dot{\hat{x}} = KG_{av}x - B_s f\varepsilon + (A_{av} - B_s F - KG_{av})\hat{x}$

and we have the observer parameters chosen in such a way that:

$A_{obs} = A_{av}, B_{obs} = B_{av}, C_{obs} = C_{av}$
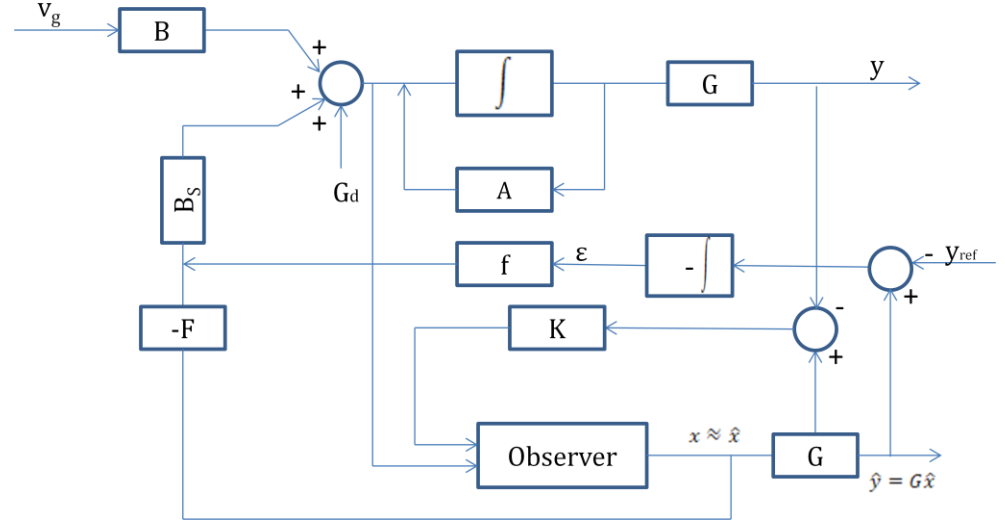
Figure 3.18 Cuk converter and full-order observer with integral action

$$\begin{bmatrix} \dot{x} \\ \dot{\varepsilon} \\ \dot{\hat{x}} \end{bmatrix} = \begin{bmatrix} A_{av} & -B_s f & -B_s F \\ G_{av} & 0 & 0 \\ KG_{av} & -B_s f & A_{av} - B_s F - KG_{av} \end{bmatrix} \begin{bmatrix} x \\ \varepsilon \\ \hat{x} \end{bmatrix} + \begin{bmatrix} B_{av} \\ 0 \\ 0 \end{bmatrix} v_g + \begin{bmatrix} G_d \\ -y_{ref} \\ 0 \end{bmatrix}$$

$$v_2 = \begin{bmatrix} G_{av} & 0 & 0 \end{bmatrix} \begin{bmatrix} x \\ \varepsilon \\ \hat{x} \end{bmatrix}$$

We have chosen arbitrarily the system initial conditions as:

$$x_0 = \begin{bmatrix} 1 & 1 & 2 & 3 \end{bmatrix}$$

The initial conditions for the observer (estimated states) are chosen using

the generalized inverse equation:

$C\hat{x}_0 = y_0 \Rightarrow C^T C\hat{x}_0 = C^T y_0 \Rightarrow \hat{x}_0 = (C^T C)^{\#} C^T y_0$ with $(C^T C)^{\#}$ as the

generalized inverse.

$$A_l = \begin{bmatrix} A_{av} & -B_s F & -B_s f \\ G_{av} & 0 & 0 \\ KG_{av} & -B_s f & A_{av} - B_s F - KG_{av} \end{bmatrix}$$

$$B_l = \begin{bmatrix} B_{av} \\ 0 \\ 0 \end{bmatrix}$$

$$G_l = \begin{bmatrix} G_{av} & 0 & 0 \end{bmatrix}$$

$$H_l = \begin{bmatrix} H_{av} \end{bmatrix}$$
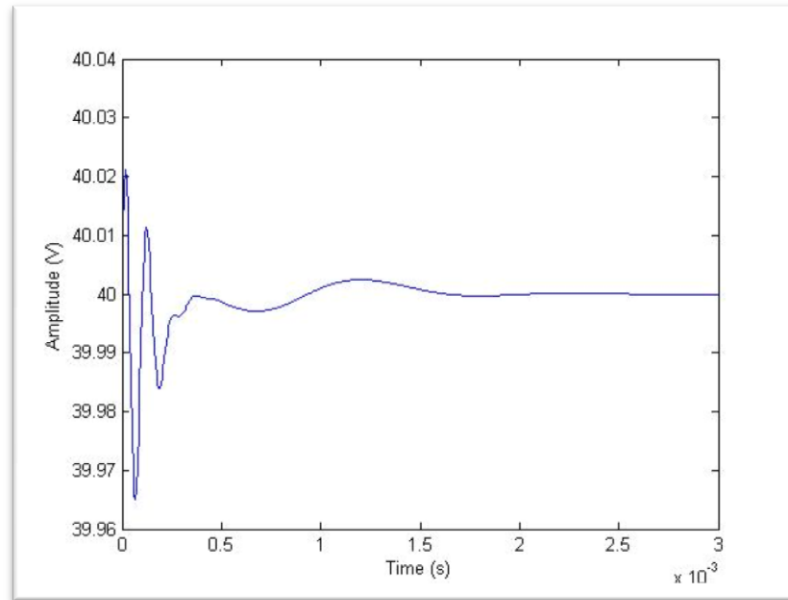
Figure 3.19 Cuk converter response with full-order observer with the integral action
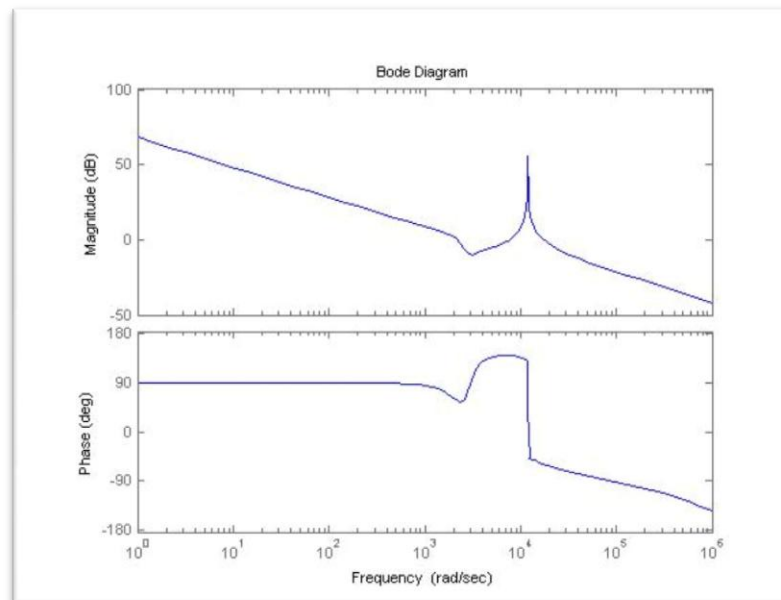
Figure 3.20 Bode diagram for the Cuk converter response with full-order observer

- Performance Loss:

The performance loss of the optimal LQ due to the use of $u = -F\hat{x}$ instead

of $u = -Fx$ can be calculated using the following expression:

$\hat{J}_{opt} = J_{opt} + J_{loss}$ with $J_{loss} = \frac{1}{2}e^T(0)P_{22}e(0) = \frac{1}{2}tr\{P_{22}e^T(0)e(0)\}$.

To avoid the dependence on the initial condition, we will consider only

$J_{loss} = \frac{1}{2}tr\{P_{22}\}$

where,

$=> (A - LC)^T P_{22} + PBR^{-1}B^T P + P_{22}(A - LC) + Q = 0$

With L being the observer gain and P obtained from the Riccati equation:

$=> A^T P - PBR^{-1}B^T P + PA + Q = 0$

We chose $Q = C^T C$ and R=3 > 0

Hence: $\hat{J}_{opt} = J_{opt} + J_{loss} = \frac{1}{2}tr\{P\} + \frac{1}{2}tr\{P_{22}\}$

In our case, the Cuk converter used with the full-order observer produces

$J_{loss} = 0.7$ and $J_{opt} = 2.76 => \frac{J_{opt} - J_{loss}}{J_{opt}} = 0.7463 => 74.63\%$ of J_{opt}

3.5.4. Reduced-Order Observer with the Integral Action

a. Reduced-Order Observer

The basic idea of the reduced-order observer is that since y is directly measured, there must be a part of the state that is also considered as directly measured; then, we should be able to build an observer of lower dimension than the full-order observer.

An observer of reduced dimensions is derived by developing the knowledge of the output measurement equation. We will assume that the output matrix C has rank p, which means that the output equation represents p linearly independent algebraic equations. Thus, equation y = Cx produces p equations of n unknown of x. So our goal will be to construct an observer with an order n−p to estimate the remaining n−p variable.

We will consider a system with the following state-space equation:

$$\dot{x} = Ax + Bu, \qquad x_0 = \text{unknown}$$

$$y = Cx = [I_p \quad 0]x$$

The system and the feedback gain can now be partitioned into measured and unmeasured portions:

$$\begin{bmatrix} \dot{x}_1 \\ \dot{x}_2 \end{bmatrix} = \begin{bmatrix} A_{11} & A_{12} \\ A_{21} & A_{22} \end{bmatrix} \begin{bmatrix} x_1 \\ x_2 \end{bmatrix} + \begin{bmatrix} B_1 \\ B_2 \end{bmatrix} u$$

$$y = x_1$$

The reduced-order state observer can be derived in a way that allows the estimation of x_2 in such a manner that all states are available for feedback via a linear control law: $u = -F_1 x_1 - F_2 \hat{x}_2$

The state variables x_1 are directly observed at all times, so that is why $y = \hat{x}_1$. To construct an observer for x_2, we use the knowledge that an observer has the same structure as the system plus the driving feedback term whose role is to reduce the estimation error to zero. Hence the observer for x_2 can be written in the following expression:

$$\dot{\hat{x}}_2 = A_{21}x_1 + A_{22}\hat{x}_2 + B_2 u + K_2(y - \hat{y})$$

Since y does not carry information about x2, the reduced-order observer will not be able to reduce the corresponding observation error to zero.

The error is defined as: $e = x_2 - \hat{x}_2$.

The reduced-order observer with the feedback information coming from the output can then be expressed in the following state-space form:

$$\dot{\hat{x}}_2 = A_{21}x_1 + A_{22}\hat{x}_2 + B_2 u + K_2(\dot{y} - \hat{y})$$

$$\dot{y} = \dot{x}_1 = A_{11}x_1 + A_{12}\hat{x}_2 + B_1 u$$

The dynamics of the estimated error is: $\dot{e} = \dot{x}_2 - \dot{\hat{x}}_2 = (A_{22} - K_2 A_{12})e$.

In order to avoid using the derivative of the output in the observer equation we introduce a change of variable: as $\hat{x}_2 - K_2 y = \hat{z}_2$, which leads to: $\dot{\hat{z}}_2 = A_q \hat{z}_2 + B_q u + K_q y$

with

$$A_q = A_{22} - K_2 A_{12}$$

$$B_q = B_2 - K_2 B_1$$

$$K_q = A_{21} - K_2 A_{11} + A_{22} K_2 - K_2 A_{12} K_2$$

The control law will be written with the change of variable as

$$u = -F_1 y - F_2 (K_2 y + \hat{z}_2)$$

thus,

$$u = -F_2 \hat{z}_2 - (F_1 + F_2 K_2) y$$

Reduced-Order Observer
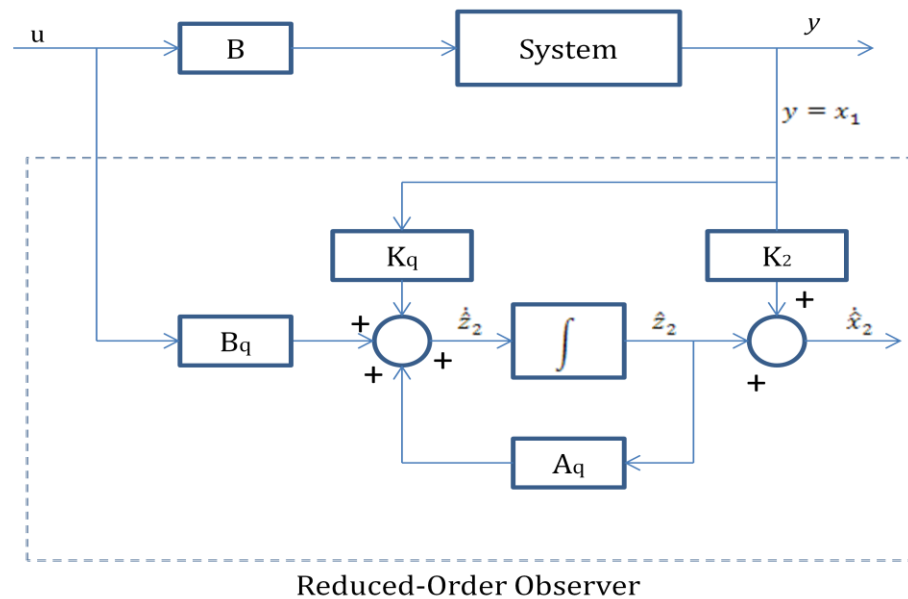
Figure 3.21 System and reduced-order observer block diagram

b. Cuk Converter with Reduced-Order Observer and Integral Action

- Implementation:

For the Cuk converter model, matrix G_{av} = [I   0] then we have i_1 as the measured state and the unmeasured states are v_1, i_2, and v_2.

Thus the reduced order observer may be designed in a way to just estimate only the three unmeasured states. The reduced order equations are given by the following state space equation:

$$\dot{x} = -B_s p_1 y - B_s p_2 \dot{\hat{x}}_2 - B_s f\varepsilon + B_{av} v_g$$

$$\dot{\hat{x}}_2 - K_2 y = \dot{\hat{z}}_2 => \hat{z} + K_2 y = \dot{\hat{x}}_2 \text{ and } y = G_{av} x$$

$$=> \dot{x} = -B_s p_1 G_{av} x - B_s p_2 \hat{z} - B_s p_2 K_2 G_{av} x - B_s f\varepsilon + B_{av} v_g$$

$$=> \dot{x} = (-B_s p_1 G_{av} - B_s p_2 K_2 G_{av}) x - B_s f\varepsilon - B_s p_2 \hat{z}$$

The integral action is $\dot{\varepsilon} = y - y_{ref} = G_{av} x - y_{ref}$

We have also $\dot{\hat{z}} = K_q y - B_q p_1 y - B_q p_2 \dot{\hat{x}}_2 - B_q f\varepsilon + A_q \hat{z}$

$$=> \dot{\hat{z}} = K_q G_{av} x - B_q p_1 G_{av} x - B_q p_2 \hat{z} - B_q p_2 G_{av} x - B_q f\varepsilon + A_q \hat{z}$$

$$=> \dot{\hat{z}} = (K_q G_{av} - B_q p_1 G_{av} - B_q p_2 G_{av}) x - B_q f\varepsilon + (A_q - B_q p_2) \hat{z}$$
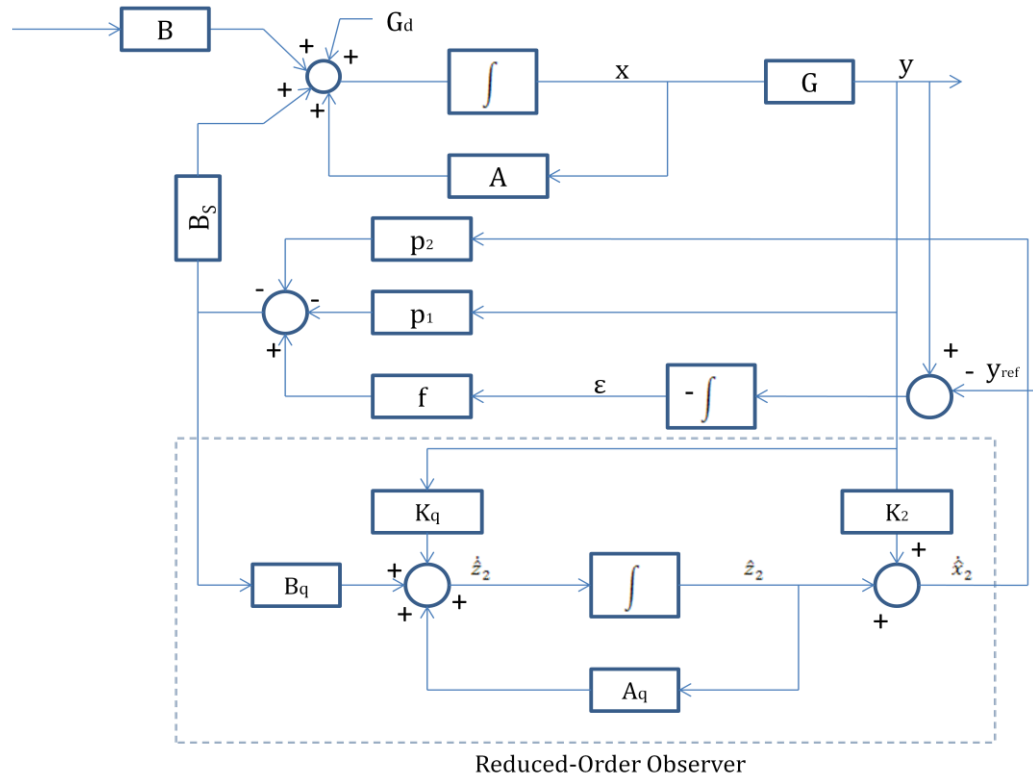
Figure 3.22 Cuk converter and reduced-order observer with the integral action

Now if we take the system that we have implemented in Section 3.5.1 (Cuk converter with integral action) and we augment it by taking care of the new reduced-order observer structure and using the formulas that we have determined in 3.5.5 part a.

We will have the augmented state-space matrices:

$$\begin{bmatrix}\dot{x}\\\dot{\varepsilon}\\\dot{\hat{z}}\end{bmatrix}=\begin{bmatrix}A_{av}-B_sp_1G_{av}-B_sp_2K_2G_{av} & -B_sf & -B_sp_2\\ G_{av} & 0 & 0\\ K_qG_{av}-B_qp_1G_{av}-B_qp_2K_2G_{av} & -B_qf & A_q-B_qp_2\end{bmatrix}\begin{bmatrix}x\\\varepsilon\\\hat{z}\end{bmatrix}+\begin{bmatrix}B_{av}\\0\\0\end{bmatrix}v_g+\begin{bmatrix}G_d\\-y_{ref}\\0\end{bmatrix}$$

$$y=[G_{av}\quad 0\quad 0]\begin{bmatrix}x\\\varepsilon\\\hat{z}\end{bmatrix}$$

$$A_l=\begin{bmatrix}A_{av}-B_sp_1G_{av}-B_sp_2K_2G_{av} & -B_sf & -B_sp_2\\ G_{av} & 0 & 0\\ K_qG_{av}-B_qp_1G_{av}-B_qp_2K_2G_{av} & -B_qf & A_z-B_qp_2\end{bmatrix}$$

$$B_l = \begin{bmatrix} B_{av} \\ 0 \\ 0 \end{bmatrix}, G_l = [G_{av} \quad 0 \quad 0] \text{ and } H_l = [H_{av}]$$

The system initial conditions are chosen as before: $x_0 = [1 \quad 1 \quad 2 \quad 3]$

The initial conditions for the estimated state are chosen using the generalized inverse equation:

$C\hat{x}_0 = y_0 \Rightarrow C^T C \hat{x}_0 = C^T y_0 \Rightarrow \hat{x}_0 = (C^T C)^\# C^T y_0$ with $(C^T C)^\#$ as the generalized inverse.

The initial conditions for $\hat{z}_2$ are: $\hat{z}_2(0) = [1 \quad 1 \quad 1]$
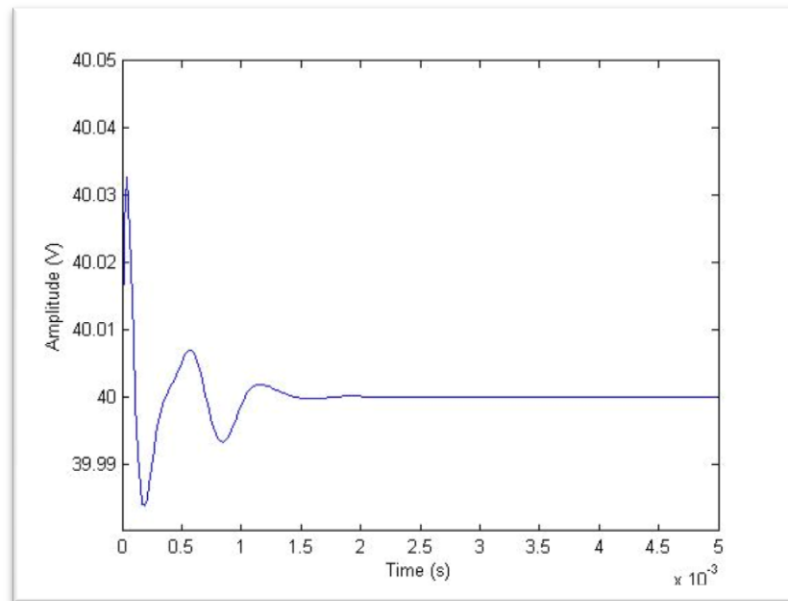
Figure 3.23 Cuk converter response with reduced-Order observer with the integral action
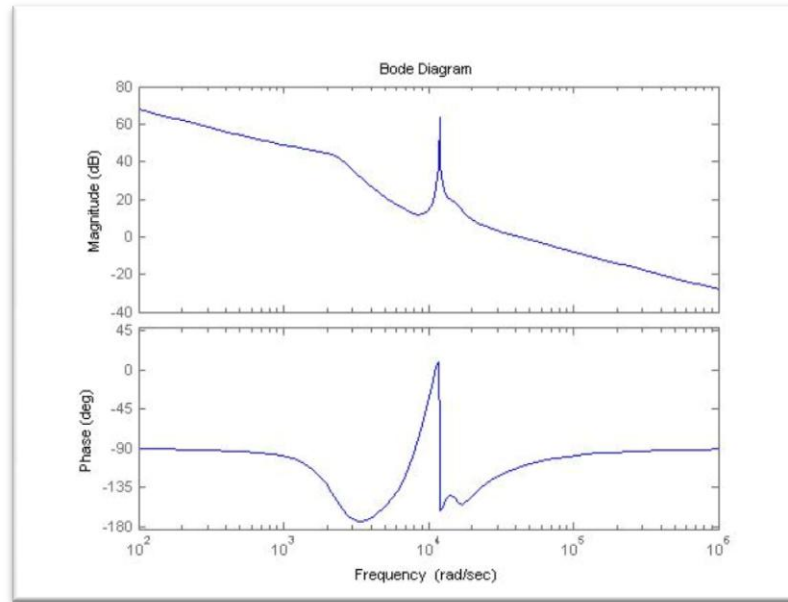
Figure 3.24 Bode diagram for the Cuk converter with reduced-order observer

- Performance Loss:

The performance loss of the optimal LQ due to the use of $u = -F\hat{x} = -Fx + Fe$:

$$\Rightarrow (A_{22} - K_2 A_{12})^T P_{22} + PB_2 R^{-1} B_2^T P + P_{22}(A_{22} - K_2 A_{12}) + Q = 0$$

with K_2 being the observer gain and P obtained from the Riccati equation:

$$\Rightarrow A_{22}^T P - PB_2 R^{-1} B_2^T P + PA_{22} + Q = 0$$

We chose Q = I and R=3 > 0.

Hence: $\hat{J}_{opt} = J_{opt} + J_{loss} = \frac{1}{2} tr\{P\} + \frac{1}{2} tr\{P_{22}\}$

In our case, the Cuk converter used with the reduced order observer hardly presents a performance loss since we have obtained $J_{loss} = 0.0185$ and $J_{opt} = 2.7671 \Rightarrow \frac{J_{opt} - J_{loss}}{J_{opt}} = 0.9933 \Rightarrow 99.33\%$ of J_{opt} which is significantly greater than that of 74.63% obtained for the full-order observer.

3.5.5. Reduced-Order vs. Full-Order Observers:

Comparing both the reduced order and the full order output response, gives us the following plot:
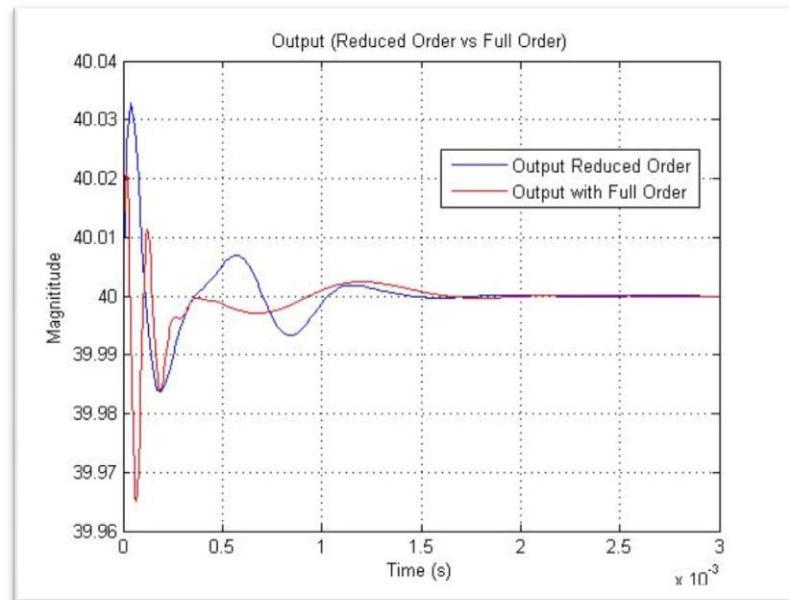
Figure 3.25 Cuk converter response (reduce-order vs. full-order)

Comparing both, reduced order and full order estimation error, gives the following plot:
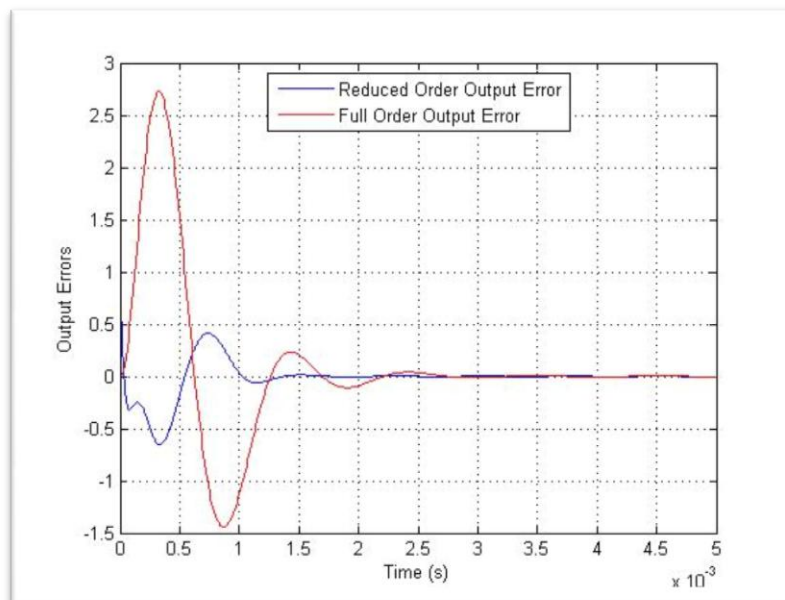
Figure 3.26 Estimation error (reduce-order vs. full-order)

We notice that the reduced order observer design presents an output response that is stabilizing relatively faster with a much better estimation error comparing to the full order observer.

Chapter 4. Maximum Power Point Tracking (MPPT)

4.1   Overview

A typical solar panel converts only around 15 percent of the incident solar irradiation into energy. In order to increase the efficiency of the solar panel we should use the Maximum Power Point Tracking technique (MPPT). According to the maximum power transfer theorem, the power delivered to the load has a maximum value when the source internal impedance (Thevenin impedance) matches the load impedance. So in other words, we need to match each time the impedance seen from the converter input side with the internal impedance of the solar panel if the system is required to operate at the MPP of the solar array.

In this thesis, as we discussed in the previous chapter, we are using, at the source side, the Cuk converter connected to the solar panel and this is a converter technique to enhance the solar array output voltage. Now by simply changing the duty cycle of the Cuk converter's switch with a smart control, we can match the source impedance with the load impedance and reach our goal. Solar panel will be then more efficient, less costly and applicable for different purposes from basic loads to non linear loads. In this way, we increase its reliability and make it more valuable for almost all residential and industrial applications.

Maximum power point tracking easiest and simplest technique is the perturb and observe method, know as P&O as well, where the controller is very easy to implement, and we need just one sensor whish is the voltage sensor to sense

the PV array voltage and the cost is a very cheap, and it is an easy model to implement. The main idea behind this controller is to provoke perturbation by acting (decrease or increase; "Hill Climbing Technique") on the PWM duty cycle command and observe the output PV power reaction.

If the actual power P (k) is greater than the previous computed one P (K-1), then the perturbation direction is maintained otherwise it is reversed (see Figure 4.1). However the method does not take account of the rapid change of irradiation level (due to which MPPT changes) and considers it as a change in MPP due to perturbation and ends up calculating the wrong MPP.

Despite the P&O algorithm is easy to implement, it cannot always operate at the maximum power point due to the slow trial and error process, and thus the solar energy from the PV arrays are not fully utilized, we have also that the PV system may always operate in an oscillating mode, and at the end the operation of PV system may fail to track the maximum power point.

To avoid this problem we can use different methods such as the incremental inductance where we sense simultaneously the voltage and the current and in this way we eliminate the previous error in the irradiance change. We have also the Fraction Open Voltage or Fraction Short Circuit techniques where we consider for the first method V_{MPP} and V_{OC} are linearly related under varying irradiance and temperature levels and for the second one I_{MPP} and I_{sc} are also linearly related as we are performing under varying atmospheric conditions.

This thesis will explain and model the advanced techniques and methods that are playing a major role in increasing PV array performance and efficiency.

4.2   Introduction to Fuzzy Logic Control Technique

4.2.1   Fuzzy Sets:

a. Definition:

A fuzzy set s is an ordered pair (X , f), where X is a vector space (usually the real line R) and f is a set membership function mapping X onto the interval [0,1] of the real line R i.e., f: $X \rightarrow$ [0,1] [16].

The set of membership function f is normalized in the sense that the value f(x) =1 is attained for at least one element x $\in$ S C X . Usually a fuzzy set is a constant construct of a time-invariant part of a fuzzy control system

The fuzzy controller design contains the three following steps [16]:

4.2.2   Fuzzification:

a. Overview: Fuzzification or coding of input variables, which transforms a given sets of numerical inputs (measured or calculated) into a fuzzy variables composed of fuzzy subsets called also membership functions. Some fuzzy subsets widely used: NB (Negative Big), NM (Negative Medium), NS (Negative Small), ZE (Zero), PS (Positive Small), PM (Positive Medium), and PB (Positive Big).

b. Definition: Consider a signal space X covered by several fuzzy sets s_i, i=1... k. The fuzzy question is: Given a vector $x \in X$, which of the fuzzy sets s_i does that x belong to? Or in which of the sets S_i associated with the fuzzy sets does x lie? In mathematical set theory, the answer is simple for each of the sets S_i is a binary one. In fuzzy set theory, set membership is "by degree". Consider a fuzzy set s=(X, f). An arbitrary element $x \in X$ belongs to the fuzzy set s with degree d=f(x). Hence our answer to the question is

that x belongs to each of the fuzzy sets s_i to some degree $d_i = f_i(x)$, i=1… k. [16]

4.2.3 Inference method or Fuzzy Logic:

a. Overview: Inference fuzzy rules or Fuzzy logic contains a set of fuzzy rules in linguistic form as well as the database which is a collection of expert control knowledge allowing achieving the fuzzy control objectives.

This control rules base can be set up using what we call the IF – THEN rules, based on expert experience and/or engineering knowledge, and learning fuzzy rule-based system which has very effective learning capabilities.

The fuzzy reasoning used to build a decision-making unit, is usually expressed as rules with AND, and OR.

b. Definitions: Consider two fuzzy sets $s_1 = (X, f_1)$ and $s_2 = (X, f_2)$ defined on the same signal space X and their associated sets $S_1 \in X$ and $S_2 \in X$.

An arbitrary element $x \in X$ belongs to the union $s_1 \cup s_2$ of the two fuzzy sets s_1 and s_2 with degree d=max $(f_1(x), f_2(x))$.

An arbitrary element $x \in X$ belongs to the union $s_1 \cap s_2$ of the two fuzzy sets s_1 and s_2 with degree d=min $(f_1(x), f_2(x))$. [16]

c. Fuzzy AND-Rules:

The AND-rule mapping the fuzzy input variables $v_{e1} = (s_{e1}, d_{e1})$ and $v_{e2} = (s_{e2}, d_{e2})$ to the fuzzy output variable $v_u = (s_u, d_u)$ is defined by $v_u = (s_u, \min(d_{e1}, d_{e2}))$.

In control engineering the definition of a fuzzy AND-rule should be: if the value $e_1(t)$ of the error signal belongs to the fuzzy set s_{e1} to degree d_{e1} and the value $e_2(t)$ of the error signal belongs to the fuzzy set s_{e2} to degree d_{e2}

then the fuzzy set s_u of the control signal is "fired" to the smaller of the two degrees, $d_u = \min(d_{e1}, d_{e2})$. [16]

4.2.4 Defuzzification:

a. <u>Overview:</u> Defuzzification of the inference engine, which evaluates the rules based on a set of control actions for a given fuzzy inputs set. This operation converts the inferred fuzzy control action into a numerical value at the output by forming the "union" of the outputs resulting from each rule. At this stage the controller has to resolve the conflict between the different rules that may "fire" at the same time. Defuzzification produces a non-fuzzy output control action that best represents the recommended control actions of the different rules.

Then, control output is compared with the saw tooth waveform to generate a PWM signal for the converter IGBT or any semiconductors switch gate command.

b. <u>Definition:</u>

The defuzzification operator D maps the fuzzy variable v_u to the centroid u of the modulate function g_u.

$$u = D\{v_u\} = D\{g_u\} = \frac{\int \propto g_u(\propto) d\propto}{\int g_u(\propto) \, d\propto} \tag{4.1}$$

Where both of the integrals are calculated over the signal place U=R. The defuzzification operator D accepts the fuzzy variable v_u as its arguments given by [17]

4.3 MPPT with Fuzzy Logic Control Technique

The fuzzy regulator has the same objectives of regulation and tracking such as a classic regulator used in automatic control theory. Recently the fuzzy logic

controllers have been introduced in the tracking of the MPP in PV systems due
to so many advantages over the regular regulators and controllers [17]:

4.3.1 Why Fuzzy Logic Controllers?

Fuzzy controllers have the advantage to be robust and relatively simple to
design and they don't require the knowledge of an accurate plant model.

4.3.2 Design and Implementation:

As we have fully describe the PV control system consists of a PV cells
connected to each other to form an array and then this array is connected
to a capacitor and then a dc/dc converter which is the Cuk converter in
our implementation. Figure 4.1 shows the entire system proposed to be
designed and implemented.
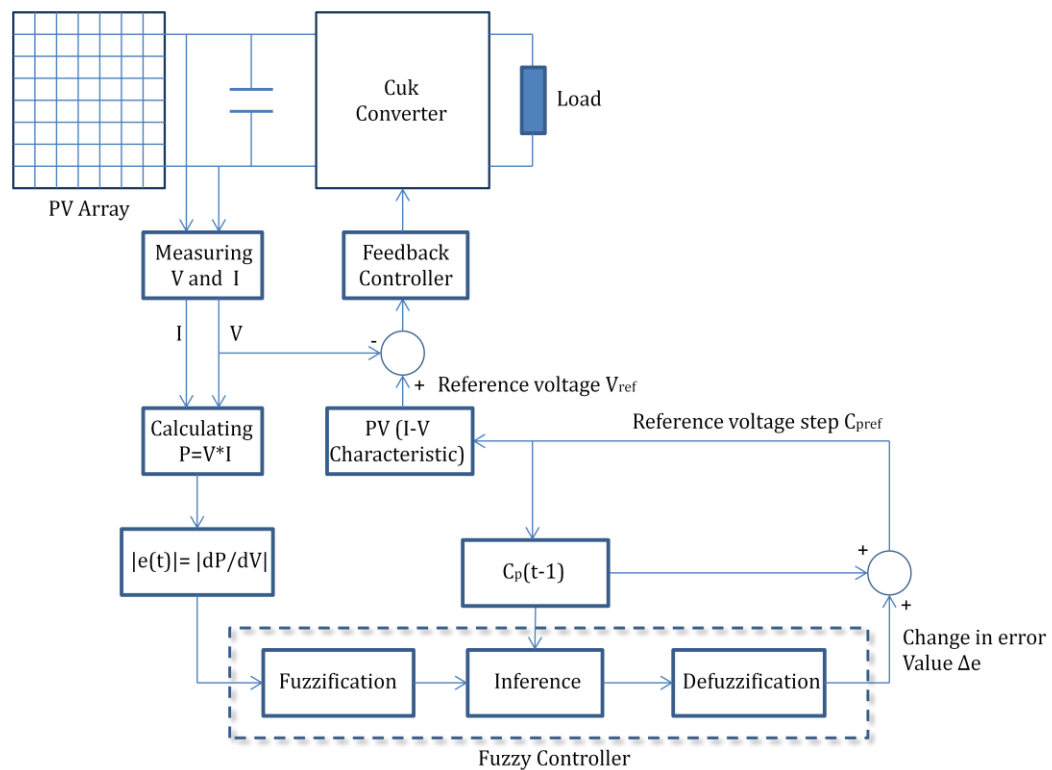
Figure 4.1 MPPT with fuzzy logic control design

The MPPT with Fuzzy logic controller architecture is based on the simple MPPT algorithm but we have added the Fuzzy technique that will increase the system efficiency and will augment the robustness of the regular MPPT algorithm. The proposed control scheme takes the absolute error e(t) of the PV panel's I-V characteristic and the (t-1) voltage perturbation C_p as inputs and calculates the change in the new change in the error Δe. The two inputs will be inserted in a fuzzification block.

After the fuzzification of the crisp inputs, the resulting fuzzy sets have to be compared to the rule-base. The rule base is a set of AND-rules created following the engineering idea that comes from the designer's experience:
If the error e(t) is Large: the operating point is definitely far from the Maximum Power Point (MPP).
Δe can then take three different values depending on C_p (t-1):

a. If C_p (t-1) is small, then the change in error Δe should be Positive Big (PB) in order to track the MPP rapidly.

b. If C_p (t-1) is medium, the change in error Δe has to be Positive Small (PS) in order to track the MPP accurately and smoothly.

c. If C_p (t-1) is big, the change in error Δe has to be Zero (ZE) in order to avid exceeding the MPP in the opposite direction.

Below are the Fuzzy Logic AND-rules values:

$C_p(t-1)$	Big	Medium	Small
$|e(t)|=\frac{dP}{dV}$	$\Delta e = C_p(t) - C_p(t-1)$		
Big	ZE	PS	PB
Medium	NS	ZE	PS
Small	NB	NS	ZE

Table 4.1 Inference method AND-rules

The last step in the fuzzy controller procedure is the defuzzification, which takes the fuzzy set and transforms it back to a crisp output.

Note: If we need to classify the MPPT techniques per their efficiency and implementation complexity in PV solar cell modeling and control, we can say that the Fuzzy Logic Control is one of the most effective techniques but it presents a higher implementation complexity than other techniques. However, the P&O, Incremental conductance, and the Fractional voltage and current have medium to low complexity but they present a lower efficiency.

4.4   Introduction to Jump Parameter Linear Optimal Control Systems

4.4.1   Overview:

Consider a linear dynamic system described by:

$$\dot{x}(t) = A(r)x(t) + B(r)u(t), \quad x(t_0) = x_0 \tag{4.2}$$

Where x(t) is the state vector of dimension n, u(t) is a control input of dimension m, A and B are mode-dependent matrices of appropriate dimensions, and r is a Markovian process that represents the mode of the system and takes on values in a discrete set $\Psi=\{1,2,...,N\}$.

The stationary transition probabilities representing the modes of the systems as the states evolve are determined by Markov chain which is the transition rate matrix given by [18]:

$$\pi = \begin{bmatrix} \pi_{11} & \pi_{12} & \cdots & \pi_{1N} \\ \pi_{21} & \pi_{22} & \dots & \pi_{2N} \\ \vdots & \vdots & \ddots & \vdots \\ \pi_{N1} & \pi_{N2} & \cdots & \pi_{NN} \end{bmatrix} \tag{4.3}$$

Markov chain is given by : $P_{k+1} = \pi * P_k$

This matrix has the property that $\pi_{ij} \geq 0$, $i \neq j$ and $\pi_{ii} = -\sum_{j \neq i} \pi_{ij}$.

The performance of the system, given by the above state space equation, is specified by the following criterion:

$$J = E\{ \int_0^\infty [x^T(t)Q(r)x(t) + u^T(t)R(r)u(t)]dt \mid t_0 , x(t_0), r(t_0)\} \tag{4.4}$$

Where:

$Q(r) \geq 0$ and $R(r) > 0$ for every r

The optimal feedback controls are then given by:

$$u_{opt} = -R_k^{-1}B_k^T P_k x(t) \qquad \text{with } k = 1, 2, \dots, N \tag{4.5}$$

Where k indicates the mode of the system:

$A(r=k) = A_k \quad B(r=k) = B_k$

$Q(r=k) = Q_k \quad R(r=k) = R_k$

And the P_k's are the positive semidefinite stabilizing solutions of a set of the coupled algebraic Riccati equations, with k=1, 2,...N:

$$A_k^T P_k - P_k S_k P_k + P_k A_k + Q_k + \sum_{j=1 \, j \neq k}^N \pi_{kj} P_j = 0 \tag{4.6}$$

Where $A_k = A_k + \frac{1}{2} \pi_{kk}I$, $S_k = B_k R_k^{-1} B_k^T$ \hfill (4.7)

Equations 4.5 and 4.6 are non-linear algebraic. The existence of positive semi-definite stabilizing solutions (stabilizable with respect to A_k) of these equations under the following assumptions

Assumption 1:

Triples $(A_i, B_i, \sqrt{Q_i})$ with i=1, 2,...N are stabilizable – detectable and

$$\left\{\begin{matrix} \inf \\ \Gamma_i \end{matrix} \middle| \lambda_{max} \left[\int_0^\infty e^{(A_i+B_i\Gamma_i+\frac{1}{2}\pi_{ii}I)^T t} x \int_0^\infty e^{(A_i+B_i\Gamma_i+\frac{1}{2}\pi_{ii}I)t}\right.\right.$$

where Γ_i are arbitrary and real matrices.

Assumption 2:

The system matrices A_k for k=1, 2...N are stabilzable by the optimal feedback control (4.4)

4.4.2   Algorithm:

Assuming that there exists a unique stabilizing $P_k \geq 0$, k=1, 2,..., N exist, the algorithm, for solving the coupled algebraic Riccati equations (4.5)−(4.6).

$$(\mathbf{A_k} - S_k P_k^{(i)})^T P_k^{(i+1)} + P_k^{(i+1)}(\mathbf{A_k} - S_k P_k^{(i)})^T = -P_k^{(i)} S_k P_k^{(i)} - \mathbf{Q_k^{(i)}} \qquad (4.7)$$

With

$$P_k^{(0)} \geq 0 \qquad k = 1,2,...,N \qquad (4.8)$$

Where

$$\mathbf{Q_k^{(i)}} = Q_k^{(i)} + \sum_{j=1\ j\neq k}^N \pi_{kj} P_j^{(i)} \geq 0 \qquad (4.9)$$

To obtain solutions of n x N order nonlinear coupled algebraic Riccati equations, we need to perform iterations on N decoupled linear algebraic Lyapunov equations each of order n.

The sequence of solutions of (4.8) and (4.9) is nested between two sequences [19].

$$K_k^{(i)} \leq P_k^{(i)} \geq \overline{P_k^{(i)}} \qquad \forall i, \forall k$$

with $\left\{K_k^{(i)}\right\}$ monotonically converging to P_k from below, that is

$$K_k^{(0)} \leq K_k^{(1)} \leq \cdots \leq P_k$$

and with $\left\{K_k^{(i)}\right\}$ monotonically converging to P_k from below, that is

$$\overline{P_k^{(0)}} \geq \overline{P_k^{(1)}} \geq \cdots \geq P_k$$

<u>Proof of Convergence:</u>

Lower Bounds: we have the following equation are the standard Riccati algebraic equations:

$$\mathbf{A_k}^T K_k^{(i+1)} + K_k^{(i+1)} \mathbf{A_k}^T + K_k^{(i+1)} S_k K_k^{(i+1)} + \mathbf{Q_k^{(i)}} = 0$$

$$\mathbf{Q_k^{(i)}} = Q_k^{(i)} + \Sigma_{j=1\ j\neq k}^N \pi_{kj} K_j^{(i)} \quad K_k^{(0)} = 0 \ , \forall k \tag{4.10}$$

It is noted that by assumption 1 the unique positive definite stabilizing solutions (4.10) exists for each iteration index i.

For i=0 we have:

$$\mathbf{A_k}^T K_k^{(1)} + K_k^{(1)} \mathbf{A_k}^T + K_k^{(1)} S_k K_k^{(1)} + Q_k = 0 \ , k = 1,2,\ldots,N \tag{4.11}$$

By assumption 1 the required positive semidefinite stabilizing solutions P_k, $k = 1,2,\ldots,N$ of (4.7) exist. Now using the results from the comparison of the solutions for the standard algebraic Riccati equations, it will follow that:

$$Q_k \leq Q_k + \Sigma_{j=1\ j\neq k}^N \pi_{kj} P_j \implies P_k \geq K_k^{(1)}$$

For i=1 , we have

$$\mathbf{A_k}^T K_k^{(1)} + K_k^{(1)} \mathbf{A_k}^T + K_k^{(1)} S_k K_k^{(1)} + Q_k + \sum_{j=1\ j\neq k}^N \pi_{kj} K_j^{(1)} = 0$$

$$Q_k + \sum_{j=1\ j\neq k}^N \pi_{kj} K_j^{(1)} \leq Q_k + \sum_{j=1\ j\neq k}^N \pi_{kj} P_j \implies P_k \geq K_k^{(2)}$$

$$Q_k \leq Q_k + \sum_{j=1\ j\neq k}^N \pi_{kj} K_j^{(1)}$$

We have that $K_k^{(1)} \geq K_k^{(2)}$

Continuing with the same procedure, we will get from (4.10) monotonically non decreasing sequences of positive semidefinite matrices bounded by P_k

These sequences are convergent and their limit points are P_k, k=1,2,3...N [19].

So we can write from the above equations that:

$$(\mathbf{A_k} - S_k P_k^{(i)})^T (P_k^{(i+1)} - K_k^{(i+1)}) + (P_k^{(i+1)} - K_k^{(i+1)})(\mathbf{A_k} - S_k P_k^{(i)})^T$$

$$= - \sum_{j=1\,j\neq k}^{N} \pi_{kj} (P_j^{(i)} - K_j^{(i)}) - (P_k^{(i+1)} - K_k^{(i+1)}) S_k (P_k^{(i+1)} - K_k^{(i+1)})$$

Upper bounds: we found that the sequences $\left\{P_k^{(i)}\right\}$ have the upper bounds in the following sequences $\left\{\overline{P_k^{(i)}}\right\} \geq \left\{P_k^{(i)}\right\}$ exist. These sequences are monotonically converging from above the required solutions of (4.5). Subtracting (4.5) – (4.7) we obtain:

$$(\mathbf{A_k} - S_k P_k^{(i)})^T (P_k^{(i+1)} - P_k) + (P_k^{(i+1)} - P_k)(\mathbf{A_k} - S_k P_k^{(i)})^T$$

$$= - \sum_{j=1\,j\neq k}^{N} \pi_{kj} (P_j^{(i)} - P_j) - (P_k^{(i+1)} - P_k) S_k (P_k^{(i+1)} - P_k)$$

If for some iterations we have $P_j^{(i)} - P_j \geq 0$ then the right hand side is negative semidefinite so that $P_k^{(i+1)} \geq P_k$ $\forall k = 1,2,3 \ldots N$ and $\forall i = 1,2,3 \ldots$

Note that the sequences $\left\{P_k^{(i)}\right\}$ are then falling between two sets of sequences:

$$\left\{K_k^{(i)}\right\} \leq \left\{P_k^{(i)}\right\} \leq \left\{\overline{P_k^{(i)}}\right\}$$

And since both $\left\{K_k^{(i)}\right\}$ and $\left\{\overline{P_k^{(i)}}\right\}$ converge to the required solution in the algorithm so will do $\left\{P_k^{(i)}\right\}$ $\forall k$. Note that both sequences $\left\{P_k^{(i)}\right\}$ and $\left\{\overline{P_k^{(i)}}\right\}$

are obtained from the same proposed algorithm and they only differ in the

initial conditions $\left\{P_k^{(0)}\right\} \le \left\{\overline{P_k^{(0)}}\right\}$, where $\left\{P_k^{(i)}\right\}$ sequences satisfy:

$$(\mathbf{A_k} - S_k\overline{P_k^{(i)}})^T\overline{P_k^{(i+1)}} + \overline{P_k^{(i+1)}}(\mathbf{A_k} - S_k\overline{P_k^{(i)}})^T = -\overline{P_k^{(i)}}S_k\overline{P_k^{(i)}} - \overline{\mathbf{Q_k^{(i)}}} \qquad (4.12)$$

with

$$\overline{P_k^{(0)}} \ge P_k \qquad k = 1,2,\dots,N \tag{4.13}$$

where

$$\overline{\mathbf{Q_k^{(i)}}} = Q_k^{(i)} + \sum_{j=1\ j\ne k}^{N} \pi_{kj}\ \overline{P_j^{(i)}} \ge 0 \tag{4.14}$$

So the initial conditions for $\left\{P_k^{(i)}\right\}$ can be chosen as arbitrary positive

semidefinite stabilizing matrices, $P_k^{(0)} \ge 0$

4.5   MPPT with a Jump Parameter Linear Optimal Controller

4.5.1   Design and Implementation:

This section of the thesis is based on applying the jump linear system

theory and the given algorithm [19] to MPPT control. The PV arrays

system state is a function of many environmental conditions like the

degree of irradiance, shadows, temperature and many others. The

efficiency of the MPPT depends on both the control algorithm chosen for

MPPT and the electrical circuitry by itself.

The Cuk converter's switch Q1 will change from mode 1 to mode 2 and

vice versa while it is tracking the Maximum Power Point of the PV array.

Thus, we will consider that this change between those systems is governed

by a Markov chain and we will apply the Jump Linear Parameter technique

to solve the coupled Riccati equation formed by these systems.

The optimal controls that minimize the performance criterion (Eq. 4.4) are then given by:

$$u_{opt} = -R_k^{-1}B_k^T P_k x \qquad \text{with} \qquad k = 1,2$$

Previously it was noted that the system is a linear dynamic one described by two state equations then, we can write that:

$$\dot{x}(t) = A(r)x(t) + B(r)u(t), \quad x(t_0) = x_0 \text{ with r=k and k=1, 2}$$

Then the

$$\pi = \begin{bmatrix} \pi_{11} & \pi_{12} \\ \pi_{21} & \pi_{22} \end{bmatrix}$$

This matrix has the property that $\pi_{ij} \geq 0$, $i \neq j$ and $\pi_{ii} = -\sum_{j \neq i} \pi_{ij}$.

Where k indicates the mode of our system:

$$A(r=k)=A_k \quad B(r=k)=B_k \qquad \text{with k} = 1, 2$$

$$Q(r=k)=Q_k \quad R(r=k)=R_k$$

and P_k's are the positive semi-definite stabilizing solutions of a set of the coupled algebraic Riccati equations, with k=1, 2:

$$A_k^T P_k - P_k S_k P_k + P_k A_k + Q_k + \sum_{j=1\ j \neq k}^{2} \pi_{kj} P_j = 0$$

where $A_k = A_k + \frac{1}{2}\pi_{kk}I$, $S_k = B_k R_k^{-1}B_k^T$

$$(A_k - S_k P_k^{(i)})^T P_k^{(i+1)} + P_k^{(i+1)}(A_k - S_k P_k^{(i)})^T = -P_k^{(i)}S_k P_k^{(i)} - Q_k^{(i)}$$

with

$$P_k^{(0)} \geq 0 \qquad k = 1, 2,$$

where

$$Q_k^{(i)} = Q_k^{(i)} + \sum_{j=1\ j \neq k}^{2} \pi_{kj} P_j^{(i)} \geq 0$$

Let's choose as a first iteration $P_k^{(0)} = 0.01 * I_4$

To obtain the required solutions from the order nonlinear coupled algebraic Riccati equations, we need to perform iterations on the two decoupled linear algebraic Lyapunov equations defined $w(k,\tau)$.

For the jump linear parameter system:

$$\dot{x} = A(1)x + B(1)u$$

$$\dot{x} = A(2)x + B(2)u$$

we choose:

$$Q_1 = Q_2 = \begin{bmatrix} 1 & 0 & 1 & 0 \\ 0 & 0 & 0 & 0 \\ 1 & 0 & 1 & 0 \\ 0 & 0 & 0 & 0 \end{bmatrix} \quad , \quad R_1 = R_2 = 1$$

and

$$\pi = \begin{bmatrix} -3 & 3 \\ 1.5 & -1.5 \end{bmatrix}$$

Using the initial condition for the Cuk converter then we will have:

$$A_1 = \begin{bmatrix} 0 & 0 & 0 & 0 \\ 0 & 0 & 130 & -130 \\ 0 & -5 * 10^5 & 0 & 0 \\ 0 & 5 * 10^4 & 0 & -1670 \end{bmatrix}$$

$$A_2 = \begin{bmatrix} 0 & 0 & -2000 & 0 \\ 0 & 0 & 0 & -130 \\ 5 * 10^5 & 0 & 0 & 0 \\ 0 & 5 * 10^4 & 0 & -1670 \end{bmatrix}$$

$$B_1 = B_2 = \begin{bmatrix} 2000 \\ 0 \\ 0 \\ 0 \end{bmatrix}$$

$$S_1 = B_1 R_1^{-1} B_1^T = S_2 = \begin{bmatrix} 4 * 10^6 & 0 & 0 & 0 \\ 0 & 0 & 0 & 0 \\ 0 & 0 & 0 & 0 \\ 0 & 0 & 0 & 0 \end{bmatrix}$$

Applying the algorithm, we obtained the following solutions with the accuracy of $O(10^{-4})$ after 6 iterations:

$$P_1 = \begin{bmatrix} 0.0015 & 0 & 0 & 0 \\ 0 & 0 & 0 & 0 \\ 0 & 0 & 0.072 & -0.0007 \\ 0 & 0 & -0.0007 & 0.0001 \end{bmatrix}, \quad P_2 = \begin{bmatrix} 0.0018 & 0 & 0 & 0 \\ 0 & 0 & 0 & 0 \\ 0 & 0 & 0.5821 & 0 \\ 0 & 0 & 0 & 0 \end{bmatrix}$$

which implies:

$$J_1^{opt} = tr\{P_1\} = 0.00736$$

$$J_2^{opt} = tr\{P_2\} = 0.5839$$

These performance criterion results show that the system is preferable to be in mode 1 and it will spend less energy to be in this mode.

Chapter 5. Thesis Conclusions and Future Research Work

5.1   Conclusions

The first chapter summarizes the basis of the research and its results. This will be followed by the plan for future research work. Summarizing the work done; photovoltaic cells (PV) were detailed, explained and studied thoroughly. An electric model for the PV cells was developed; I-V characteristics were plotted per the irradiance values and the effects of weather and shadows was detailed. The operation of a photovoltaic (PV) cell requires 3 basic attributes: absorption of light, generating either electron-hole pairs, and separation of various types of charge carriers and the separate extraction of those carriers to an external circuit

The third chapter discussed the Cuk converter as one of the thesis' key features. Average and dynamic state space matrices were identified, a state space analysis from open loop to regular and simple closed loop were also studied. MATLAB/SIMULINK software was used to plot the output values and check the Cuk converter behavior under disturbance and input variance. The Cuk converter was also studied with control strategies like the full state feedback control with and without integral effort. The thesis contribution was by simulating the Cuk converter using estimation techniques with full and reduced-order observers adding to them the integral action to make it more and more competent and efficient. Great results were demonstrated with a very high performance, making Cuk one of the best converters to simulate and to install with a PV system because we can achieve our goal of high efficiency.

The thesis also discussed two major and efficient control techniques for the Maximum Power Point Technique (MPPT); the Fuzzy Control and its high reliability with very dynamic and weather related systems and the Jump linear technique with an efficient algorithm.

5.2   Future Research Work

Future work will simulate a non linear model of Cuk converter with parasitic components and will seek to sample the Cuk converter's switch duty cycle. The new simulated model will be then very close to reality.

Future research work will also model the PV array with the Jump linear technique applied to the Cuk converter for Maximum Power Point tracking. The Cuk converter shall also include the reduced order observer with integral action control strategy to maximize the system's efficiency.

The research work and if the results were also successful as they are manifested theoretically, can be engineered and sent out for physical testing and prototype production.

References

[1]. Kosuke Kurokawa, "Energy from the Desert", 2003.

[2]. C.J.Winter, R.L. Sizmann, L.L. Van-Hull, "Solar Power Plants", 1991.

[3]. European Photovoltaic Industry Association (EPIA), Rue d´Arlon 63-65 1040 Brussels – Belgium, "Global Market Outlook for Photovoltaics until 2012 Facing a sunny future", p. 4, Figure 4: "Regional distribution of global PV markets (Policy Driven Scenario)", 2012.

[4]. Adolf Goetzberger, Volker U. Hoffmann, "Photovoltaic Solar Energy Generation", Springer Berlin Heidelberg New York, 2005.

[5]. Stuart R. Wenham, Martin A. Green, "Applied photovoltaic", Earth Scan, 2007.

[6]. Falk Antony, Christian Durschner, "Photovoltaic for Professionals", Earth Scan, 2007.

[7]. John Twidell and Anthony D. Weir, "Photovoltaic Generation", 2006

[8]. Robert W. Erickson and Dragan Maksimovic, "Fundamentals of Power Electronics", Second Edition, University of Colorado, Boulder, 2001.

[9]. Slobodan Cuk , R. D. Middlebrook, "Advances in Switched-Mode Power Conversion Part I", p. 10 – 19, Feb 1983

[10]. R. D. Middlebrook and S. Cuk, "A general unified approach to modeling switching-converter power stages", 196 IEEE Power electronics Specialists Conference Record, 196, p. 18-34, 1973.

[11]. Gabriel Oliver Codina, "Linear State Feedback Control Laws", Systems, Robotics & Vision Group Universitat de les Illes Balears, 2006.

[12]. L.J Nagrath and M. Gopal, "Control Systems Engineering", 2006.

[13]. Brian. D. O. Anderson and J. B. Moore, Optimal Control, "Linear Quadratic Methods", Englewood Cliffs, NJ: Prentice Hall, Inc., 1990.

[14]. Donald E. Kirk," Optimal Control Theory: An Introduction", The Dover Edition, published by Prentice-Hall, Inc., Englewood Cliffs, New Jersey , 1970.

[15]. Z. Gajic and M. Lelic, "Modern Control Systems Engineering", Prentice Hall International, London, 1996, (pages 241–247 on full- order observers).

[16]. Sofai. Lalouni, Djamila. Rekioua, "Modeling and Simulation of Photovoltaic System using Fuzzy Logic Controller", IEEE International Conference on Developments in Systems Engineering, p. 23 – 28, 2009.

[17]. Hans P. Geering," Introduction to Fuzzy Control: IMRT Press Measurement and control laboratory", Swiss Federal Institute of Technology, ETH-Zentrum, CH-8092 Zurich, Switzerland, 3rd edition, September 1998.

[18]. M. Mariton," Jump Linear Systems in Automatic Control", New York: Marcel Decker, 1990.

[19]. Z. Gajic and I. Borno, "Lyapunov Iterations for Optimal Control of Jump Linear Systems at Steady State", IEEE Transactions on Automatic Control, Vol. 40, No. 11, p. 1971 – 1975, November 1995.